Report No. BMI-1322
C-83 - Reactors - Special Features of Military Package Power Reactors (M-3679, 22nd Ed., Rev. 1)

Contract No. W-7405-eng-92

THE EFFECT OF FABRICATION VARIABLES ON THE STRUCTURE AND PROPERTIES OF UO_2-STAINLESS STEEL DISPERSION FUEL PLATES

by

Stan J. Paprocki
Donald L. Keller
George W. Cunningham

February 18, 1959

RESTRICTED DATA

BATTELLE MEMORIAL INSTITUTE
505 King Avenue
Columbus 1, Ohio

DISCLAIMER

TABLE OF CONTENTS

THE EFFECT OF FABRICATION VARIABLES ON THE STRUCTURE AND PROPERTIES OF UO_2-STAINLESS STEEL DISPERSION FUEL PLATES

Stan J. Paprocki, Donald L. Keller, and George W. Cunningham

Based on the results of detailed fabrication studies, an evaluation of the effects of varying the type and size of UO_2 particles, the type and size of stainless steel matrix powders, blending procedures, compacting pressures, sintering times, temperatures, and atmospheres, roll-cladding temperatures and reduction rates, total cold reduction, and heat-treating times and temperatures has been made for UO_2-stainless steel dispersion fuel elements. Transverse tensile tests, creep-rupture tests, metallographic examination, radiography, density measurements, and X-ray diffraction studies were used to evaluate the structure and properties of the fuel elements.

From these studies a reference fabrication procedure for GCRE fuel elements was established. The fuel element core contains 30 w/o of minus 100 plus 200-mesh hydrothermal UO_2 dispersed in an 18-14-2.5 alloy matrix prepared from minus 325-mesh elemental iron, chromium, nickel, and molybdenum powders. Commercial Type 318 stainless steel is used for cladding. Core compacts are sintered in steps to 2300 F after cold compacting at 15 tsi. Evacuated picture-frame packs are hot rolled from a hydrogen muffle at 2200 F with a 40 per cent reduction in thickness on the first pass and a 20 per cent reduction in thickness on remaining passes. After annealing at 2300 F, the fuel elements are given a light pickle and cold reduced 15 to 20 per cent in thickness to give a total reduction of 8 to 1. The final treatment consists of a flat anneal at 2050 F.

INTRODUCTION

This report deals with a part of the research and development studies which preceded the manufacture of fuel elements for the Gas Cooled Reactor Experiment (GCRE). A GCRE fuel element will be prepared by die forming, through 120 deg, twelve stainless steel-UO_2 fuel plates of four different widths which are subsequently assembled into four concentric tubes. Each plate is 0.045 in. thick, while the active core is 0.033 in. thick and 28 in. long. Three formed plates making up each individual tube will be held together mechanically by three clips running the full length of the element. These clips will also space the tubes with respect to each other and to the tubular insulation lining and thus form the appropriate passages for the gas coolant. The inside diameter of the outer and inner fuel tube is approximately 1.2 in. and 0.5 in., respectively. The inside diameter is particularly important since it presented a die-forming problem which ultimately led to the selection of elemental powders as the fuel-element matrix material.

The average maximum fuel-element surface temperature anticipated in the GCRE is about 1400 F, while hot-spot temperatures are expected to reach 1650 F. The gas coolant will be nitrogen plus a small amount of oxygen to inhibit corrosion. The results from the detail corrosion studies reported elsewhere contributed to the selection of Type 318 stainless steel as the cladding material. Other factors considered in this selection were the high-temperature strength of Type 318 stainless steel as well as its fabricability and availability.

Throughout the fuel-element development studies it was recognized that an element possessing outstanding radiation stability would be required to fulfill the lifetime and operating-temperature requirements imposed by the GCRE. A great deal of attention, therefore, was given to the many processing variables encountered during the fabrication of stainless steel-UO_2 dispersion elements in hopes of "paving the way" toward the manufacture of elements possessing optimum characteristics.

It is demonstrated throughout this report just how dependent the mechanical properties are upon the methods used during fabrication. It is further believed that those same operations which adversely affect the mechanical properties of this type element, particularly the transverse tensile strength, will also lower its resistance to radiation damage. This is presently being demonstrated in a series of GCRE irradiation experiments and will be the subject of later reports.

In an effort to obtain an optimum structure, a large number of variables have been investigated. Factors which have been considered include selection of core materials and the determination of fabrication temperatures, reduction rates, powder particle sizes, and core-preparation methods. The evaluation of these variables has been based upon results of microscopic and macroscopic examinations which have been correlated with results of physical- and mechanical-property tests. In particular, the transverse tensile test (tensile strength measured in the plate-thickness direction) has been found to be useful in evaluating fabrication variables. Other mechanical-property tests employed include hot tensile, stress-to-rupture, and bend tests. In addition, radiography has proven to be a useful tool in evaluating mixing, compacting, and rolling procedures.

The selection of a core-matrix material could not be made until both prealloyed stainless steel powders and stainless steel made from mixtures of iron, chromium, nickel, and molybdenum powders were evaluated. Therefore, this report contains the results of the development studies on both types of materials, and methods are described for obtaining optimum core structures with either core matrix. Recommended fabrication procedures are listed in Appendix A.

Since maximum stringering and fracturing of UO_2 occurs in the direction of rolling, fuel elements must be sectioned in a direction parallel with the rolling direction if fabrication variables are to be evaluated. Therefore, unless otherwise indicated, all photomicrographs were made of longitudinal sections.

PREPARATION OF GREEN COMPACTS

The structure, distribution of UO_2, density, and shrinkage of the sintered core are partially controlled by the method of preparing green compacts. Variables which were investigated include blending procedures, selection and use of a binder and die lubricant, die design, and cold-compacting pressures.

Materials

The compositions of metal powders used in this investigation are listed in Table 1. Core matrices of the three stainless steels studied (Types 302B, 347, and 318) were prepared from both prealloyed stainless steel powders and mixtures of elemental iron, chromium, nickel, and molybdenum powders. Most of the experimental work was carried out with Type 318 stainless which was selected as the fuel-element matrix and cladding material because of its comparatively high creep strength and its resistance to oxidation and nitriding at GCRE operating temperatures.

Strong, dense, crystalline particles of UO_2 are required for producing good dispersions. Mallinckrodt Hi-Fired UO_2 was used as the prototype fuel material. This UO_2 shows a high degree of crystallinity, nearly zero porosity, and a uranium-to-oxygen ratio of very nearly the stoichiometric value. It is prepared by adding a small amount of TiO_2 (approximately 0.7 w/o) to the UO_2 and firing at a temperature high enough to cause a somewhat vitreous phase (probably rich in TiO_2) to form at the grain boundaries and thus draw the individual grains into a dense particle. Hydrothermal UO_2 produced at Oak Ridge by hydrogen reduction of crystals grown from a UO_3 hydrate-uranyl nitrate solution was used in the fabrication of fuel elements requiring fully enriched UO_2. These particles also show a high degree of crystallinity and are very dense, and, in addition, they more nearly resemble fused UO_2 particles than the Hi-Fired UO_2. Recently a spherical UO_2 powder has been made available by Mallinckrodt, but only a limited amount of work with this powder could be conducted before the completion of the program. Poor results obtained with other types of UO_2 were previously reported[1]; therefore, most of the development work was conducted with Hi-Fired and hydrothermal UO_2.

Petrographic analyses of Hi-Fired, spherical, and hydrothermal UO_2 are listed in Table B-1 in Appendix B.

Blending

The blending of the compacts containing prealloyed Type 318 powders was similar to the method used for blending compacts containing elemental iron, chromium, nickel, and molybdenum powders with the exception that the prealloyed powder did not have to be blended prior to adding the UO_2. Comparison of the various mixers has clearly shown the advantage of using a twin-shell V-type blender. In a rotating cylinder the powder may simply slide around the walls without mixing. In the obliquely rotating cylinder blending is somewhat improved since the powder is thrown from end to end, but best results are obtained with the twin-shell blender, which throws the powder, mixes it, and divides it. The addition of baffles, screens, or balls will improve the mixing action of the single cylinders, but there will also be a tendency for the brittle UO_2 to be ground or fragmented. If UO_2 is not present in the batch, a screen can also be added to the twin-shell blender to improve the mixing of the metal powders.

(1) References at end.

TABLE 1. CHEMICAL COMPOSITION OF

	Analyzed Compo-							
	Fe	Cr	Ni	Mo	Si	Mn	Mg	Cu
Carbonyl iron	Bal	0.005	0.5	0.01	0.005	0.005	0.01	0.01
Electrolytic iron	Bal	0.001	0.1	0.005	0.001	0.005	0.005	0.03
Hydrogen-reduced electrolytic iron	Bal	0.001	0.1	0.005	0.001	0.005	0.005	0.03
Lunex chromium	0.01	Bal	0.005	0.01	N.D.	0.01	0.002	0.03
Electrolytic chromium	0.01	Bal	N.D.	N.D.	0.001	0.005	0.005	0.01
Carbonyl nickel	0.1	0.005	Bal	N.D.	N.D.	N.D.	N.D.	N.D.
Molybdenum	0.01	N.D.	0.01	Bal	0.001	N.D.	N.D.	N.D.
Type 302B stainless	Bal	18.94	8.77	--	2.36	0.98	--	--
Type 347 stainless (high silicon)	Bal	18.62	11.44	--	2.35	1.56	--	--
Type 318 stainless	Bal	18.20	11.31	2.34	2.44	0.01	--	--

(a) Analyses on prealloyed powders furnished by Vanadium Alloys Co.
N.D. = not detected; Bal = balance.

METAL CORE-MATRIX POWDERS

sition[a], w/o								
Ce	Al	Ca	C	S	P	O_2	H_2	N_2
N.D.	0.05	0.05	0.08	0.006	0.003	0.1680	0.0020	0.0024
0.01	0.01	N.D.	0.01	0.017	0.004	0.6050	0.0020	<0.0010
0.01	0.01	N.D.	0.01	0.017	0.004	0.2000	0.0004	<0.0010
N.D.	N.D.	N.D.	0.10	0.006	0.001	0.0995	0.0019	0.0029
N.D.	0.02	N.D.	0.05	0.021	0.002	0.7110	0.0150	<0.0070
N.D.	N.D.	N.D.	0.04	0.005	0.001	0.0425	0.0023	0.0025
N.D.	0.1	N.D.	0.01	0.003	0.006	0.2770	0.0031	0.0900
--	--	--	0.08	0.028	0.013	--	--	--
--	--	--	0.05	0.011	0.017	--	--	--
--	--	--	0.10	0.008	0.021	--	--	--

The use of a binder or internal lubricant is necessary to insure a uniform distribution of UO_2. The UO_2 particles, which are not only larger but also of a higher density, tend to segregate when mixed with the stainless steel powder. When a binder such as a camphor-alcohol solution is added there is a tendency for the individual UO_2 particles to be coated with the binder and thus be held in suspension in the metallic matrix. On the other hand, if improperly added, the binder can also cause segregation. For example, if added at the same time as the UO_2, the binder can cause the UO_2 particles to be agglomerated, as indicated in Figure 1. There are several binders which can be used satisfactorily, but the binder selected should either evaporate at a low temperature or decompose during the sintering operation in such a manner that no impurities are added to the core compact. Some of these materials are ashless wax solutions, camphor solutions, stearic acid, and zinc stearate.

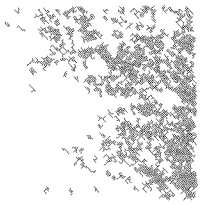

1X F512

FIGURE 1. POSITIVE PRINT MADE FROM RADIOGRAPH OF ROLL-CLAD SPECIMENS OF 25 w/o UO_2 IN 18-14-2.5 ALLOY

Specimen at left was mixed dry before binder was added. In the right specimen the binder and UO_2 were added simultaneously.

If elemental powders are used, the blending procedure must also provide for a homogeneous distribution of the nickel, chromium, and molybdenum in the iron powder. To achieve this result the powders must be mixed dry before the UO_2 is added. Screening of the powder before mixing is necessary not only to size the powder but to break up agglomerates. It is also advantageous to screen the powder mix at some intermediate point during the blending. Examination of the microstructures shown in Figure 2 shows that a homogeneous austenitic matrix is easier to obtain if the stainless powder is properly blended before adding the UO_2. When the metal powders are not screened and blended before adding UO_2, chromium agglomerates and is difficult to get into solution; also, the UO_2 agglomerates if not mixed with dry powders. Both specimens in Figure 2 were fabricated by identical procedures.

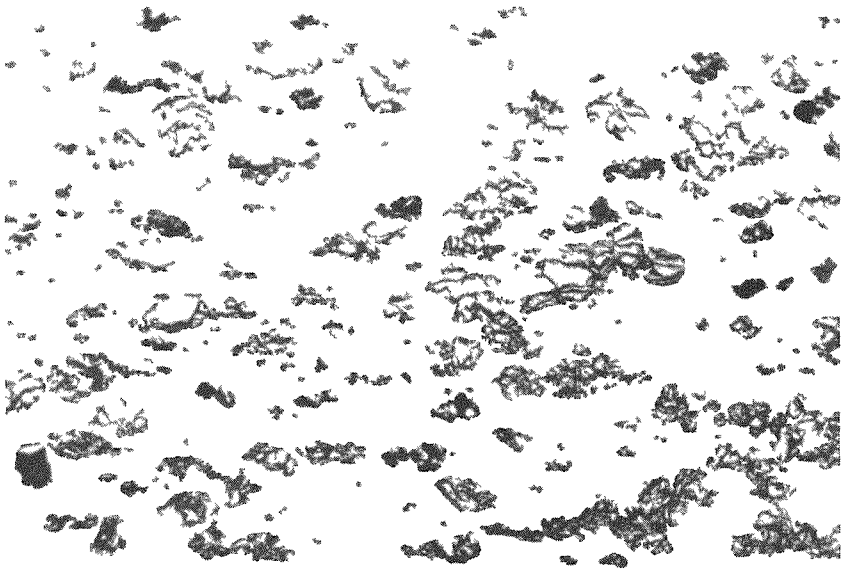

100X Glyceria Regia Etch N46782

a. Metal Powder and UO_2 Mixed Separately

Metal powders blended dry 1/2 hr, screened, blended 1 hr, UO_2 and binder added simultaneously. Note homogeneous matrix but agglomerated UO_2.

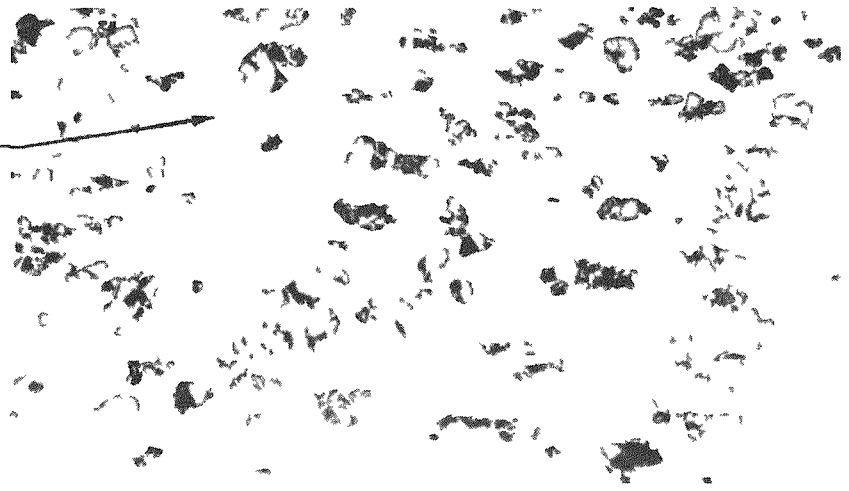

100X Glyceria Regia Etch N46786

b. Metal Powder and UO_2 Mixed Simultaneously

Metal powders and UO_2 blended dry for 2 hr without previous blending of metal powders and 2 hr after addition of binder. Note less agglomeration of UO_2, but presence of chromium-rich areas.

FIGURE 2. EFFECT OF BLENDING PROCEDURE ON STRUCTURE OF ROLL-CLAD 25 w/o UO_2 IN 18-14-2.5 ALLOY

Transverse sections.

Cold Pressing

After the powders were properly blended, the weighed portions were cold pressed. The length and width dimensions of the pressed compact were approximately 0.010 in. larger than the die punch, depending upon the compacting pressure. The thickness of the compact was regulated by the quantity of material used and the compacting pressure. When pressing rectangular compacts such as those used for GCRE fuel plates, it was necessary to spread the powder evenly in the die cavity to obtain a uniformly thick compact. A 50-tsi pressure was used to press compacts with a prealloyed stainless steel matrix and a 15-tsi pressure was used for the compacts with an elemental stainless steel matrix in most of the work. The higher pressure was desirable with prealloyed-matrix compacts because higher final densities would be obtained, but the low pressure was used with the elemental-powder compacts to decrease the initial density and thus promote the hydrogen reduction of any oxides present during the sintering operation. A detailed discussion of oxide reduction is included in the section on sintering.

For experimental work, it was found more desirable to use a split-type die (Figure 3) rather than an ejection-type die since in many cases the ejection pressure can be greater than the compacting pressure. Although the use of a double-acting or floating die is advantageous for producing compacts of a uniform density, it is not necessary for pressing thin compacts. In fact, the uniformity is more dependent upon uniform loading of the die. Mechanical vibration was not satisfactory for leveling the powder. Such an action tends to segregate the UO_2. The best method consists of adjusting the die so that the top of the fill is even with the top of the die. The bottom punch is then lowered, the top punch inserted, and the powder is pressed. The effect of compacting pressures on the green strength as related to handling for both prealloyed and elemental powders is shown in Table 2.

SINTERING

The sintering of stainless steels is far more complex than the sintering of pure metals. The only problem in producing dense bodies from pure metal powders consists of bonding the individual particles and shrinking the voids to a low volume per cent. The final density which can be attained will be due to the rate of self-diffusion or creep at the sintering temperature, but the final pore size will also be limited to a size at which the force exerted by entrapped gas equals the force due to surface tension.[2] In practice, densification of single-metal compacts occurs at a low rate after 2 to 4 hr at temperature, but much longer times are required to produce homogeneous alloys from mixtures of iron, chromium, nickel, and molybdenum powders. Diffusion rates should be similar to those obtained in standard diffusion couples, but the rates can be greatly affected by the presence of absorbed gases or oxide films, intermediate-phase formation, and reaction with other impurities. In addition, the surface area in contact with the base metal as determined by particle size and green density has a direct influence on the diffusion rate. Even when prealloyed stainless steel powders are used, the presence of impurities such as carbon and silicon can cause the formation of secondary phases. Futhermore,

the porosity is usually greater than would be expected in the elemental mixtures. The stainless steel powder is basically harder than the iron and nickel powders and, in addition, the hardness is increased by work-hardening effects which may even occur in mixing. This increased hardness prevents plastic flow to a certain extent and thus decreases the contact areas of the particles; consequently, the green strength and sintered density are decreased.

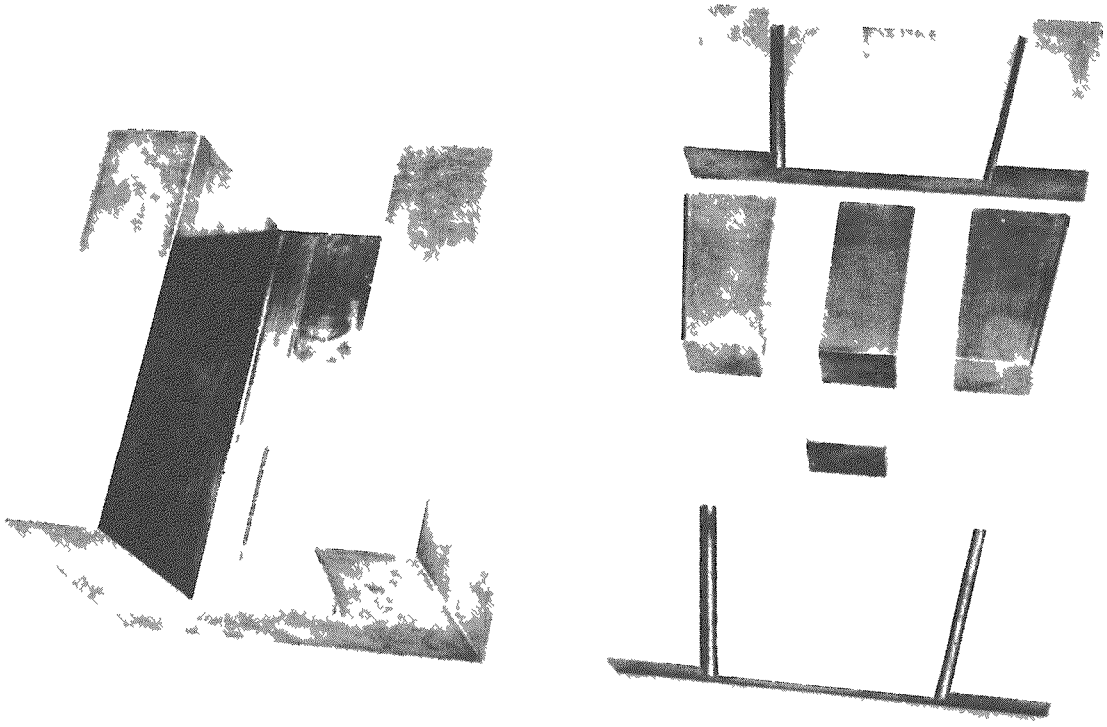

1/2X N38035

FIGURE 3. SPLIT-TYPE COMPACTING DIE

Elemental Mixtures

The use of chromium is the cause of two major difficulties in sintering elemental mixtures to produce an austenitic stainless steel structure. The first problem occurs because complex sintering procedures are necessary to reduce Cr_2O_3, while the second problem arises from the fact that chromium is the most difficult constituent to get into solution. Of these two problems, the reduction of Cr_2O_3 was the most troublesome to solve.

An examination of Table 1 shows that of commercially available powders only electrolytic chromium and electrolytic iron have excessively high values of oxygen. In electrolytic chromium with 0.6 to 0.8 w/o oxygen, there could be up to 3.5 volume per cent Cr_2O_3, which if not reduced during sintering would result in approximately

TABLE 2. RESISTANCE OF GREEN COMPACTS TO DAMAGE BY HANDLING[a]

Composition	Compacting Pressure, tsi	Density, per cent of theoretical	Weight Loss After Indicated Testing Time, per cent		
			5 Min	15 Min	30 Min
Elemental 18-14-2.5 alloy[b]	15[c]	63.0	7.6	17.9	32.2
	25[d]	69.6	3.04	6.34	11.15
	35[c]	74.9	1.26	2.53	4.55
	50[c]	79.1	0.75	1.50	2.51
Prealloyed Type 318 stainless steel	15[c]	Too fragile to measure	100.0	--	--
	25[c]	Too fragile to measure	100.0	--	--
	35[c]	Too fragile to measure	100.0	--	--
	50[c]	70.5	100.0	--	--
	50[d]	66.5	59.0	--	--

(a) Compacts for each composition and fabrication condition were placed on an 80-mesh screen and run in a Tyler Rotap for the indicated time.
(b) Iron 18 w/o chromium-14 w/o nickel-2.5 w/o molybdenum.
(c) Camphor-methanol binder.
(d) Methyl-cellulose binder.

0.7 volume per cent Cr_2O_3 in an 18-8 stainless steel. Oxygen in iron, if not removed by reaction with hydrogen, can also react to form Cr_2O_3. For example, as shown in Figure 4, high-purity crystal-bar chromium reacted with iron containing 0.7 w/o oxygen to form Cr_2O_3. Up to 3 volume per cent Cr_2O_3 in stainless steel could be produced by the iron powder. On the other hand, commercially produced nickel and molybdenum powders did not promote the formation of Cr_2O_3. Specimens of iodide chromium dispersed in nickel (0.042 w/o oxygen) or molybdenum (0.277 w/o oxygen) sintered at the same time as the iron-chromium specimen mentioned above did not contain any detectable Cr_2O_3. As further evidence that Cr_2O_3 is present or forms during sintering from oxygen in the metal powders, compacts sintered for 4 hr in vacuo at 2250 F contained Cr_2O_3.

Usually the final step in the production of electrolytic iron powder is a hydrogen anneal which reduces the oxygen content, but after long periods of storage the oxygen content may again approach 0.8 w/o. A 1-hr anneal at 1200 F shortly before use will reduce the oxygen to approximately 0.2 w/o. Carbonyl iron powder as received has less oxygen than as-received electrolytic iron powder, but the carbon content (0.08 w/o) may be higher than desired. The use of a low-oxygen iron powder is more important than using a low-oxygen chromium powder such as Lunex lithium-reduced powder, but a complex sintering procedure and a very dry hydrogen atmosphere are required in both cases.

The reduction of the Cr_2O_3 may be represented by the equation

$$Cr_2O_3(c) + 3\,H_2(g) \rightarrow 2\,Cr(c) + 3\,H_2O(g).$$

According to thermodynamic data, the products and reactants are in equilibrium at 2000 F with a dew point of -25 F and at 2300 F with a dew point of -2 F. However, the hydrogen furnace exit dew points must be maintained at a considerably lower level. Figure 5 shows how the dew point varied with time and temperature in several typical runs. All compacts sintered in atmospheres in which the dew point did not exceed -30 F and recovered to less than -40 F after 2 hr at 2300 F were free from Cr_2O_3. When the dew point exceeded -5 F and did not recover to less than -15 F, all compacts contained Cr_2O_3. If in sintering the maximum dew point was -10 F and it recovered to less than -20 F, the amount of Cr_2O_3 was small and in some cases all the Cr_2O_3 was reduced. In all tests the hydrogen which entered the furnace had a -100 F dew point.

The reduction of the Cr_2O_3 is not only dependent upon the dew point but also indirectly upon the compacting pressure. At temperatures high enough for the Cr_2O_3 to be reduced, the stainless steel sinters and pores are closed off which permit easy flow of hydrogen into the compact and passage of water vapor out. Thus dew points which ordinarily would provide a sufficient driving force for the Cr_2O_3 reduction may not be representative of conditions within the compact. However, if compacts are pressed at low enough pressures, it may be possible to reduce the Cr_2O_3 before extensive sintering takes place. The data listed in Table 3 and the microstructures in Figure 6 show the effect of compacting pressure as related to the presence of Cr_2O_3 and to the final density obtained.

The actual dew point required may also be considered as dependent upon the cold compacting pressure. If the dew point is sufficiently low, all the Cr_2O_3 can be reduced

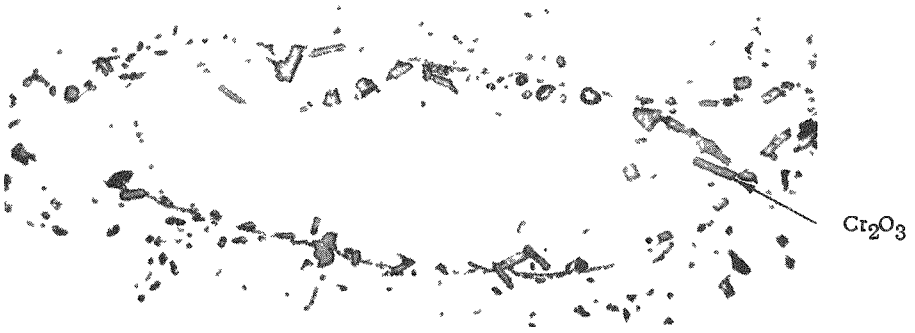

100X Oxalic and NaCN Etch N50815

a. Electrolytic Iron Matrix (0.7 w/o Oxygen)

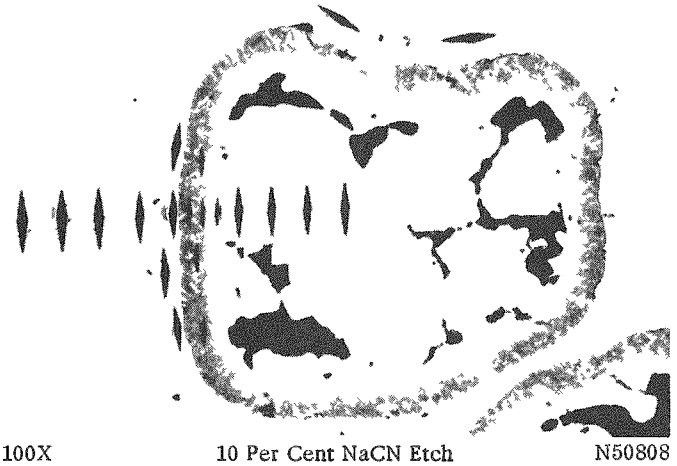

100X 10 Per Cent NaCN Etch N50808

b. Carbonyl Nickel Matrix (0.042 w/o Oxygen)

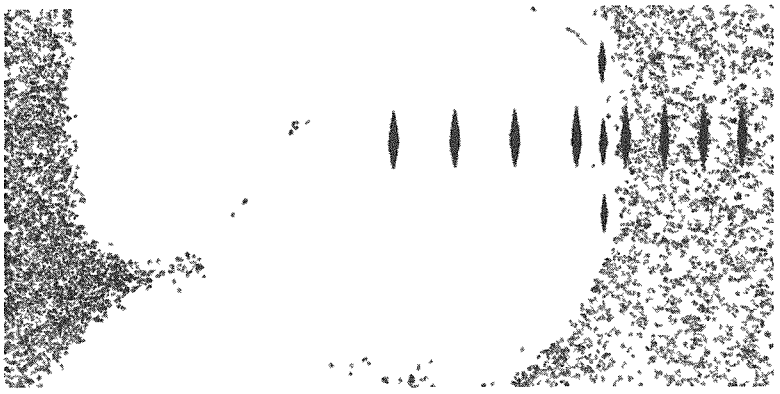

100X 10 Per Cent NaCN Etch N50809

c. Hydrogen-Reduced Molybdenum Matrix (0.277 w/o Oxygen)

FIGURE 4. EFFECT OF OXYGEN IN 18 w/o IODIDE CRYSTAL-BAR CHROMIUM POWDER COMPACTS

Note that diffusion zones can be seen in all specimens but Cr_2O_3 is present only in the iron-matrix specimen.

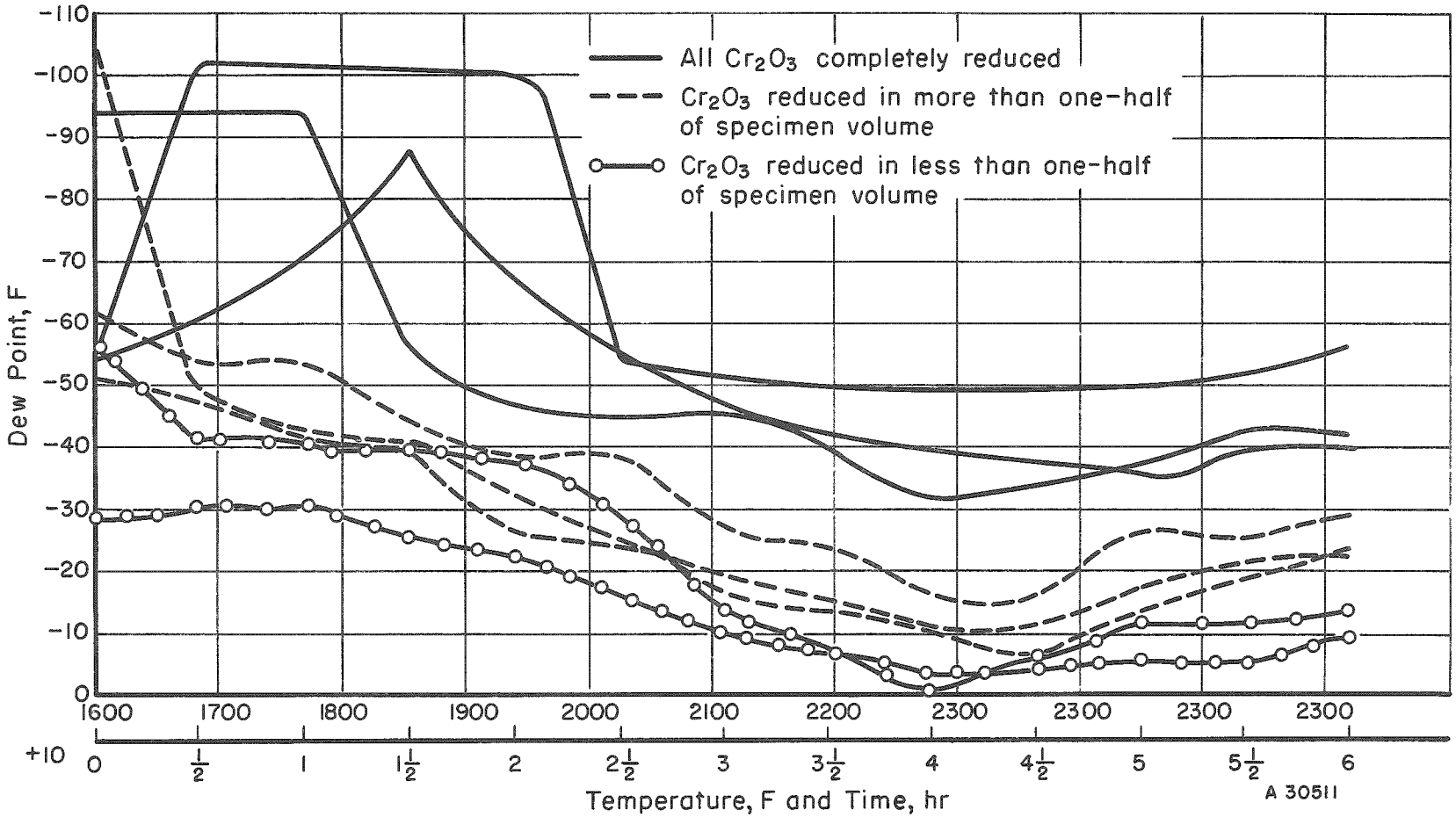

FIGURE 5. VARIATION OF DEW POINT WITH TIME AND TEMPERATURE FOR TYPICAL SINTERING RUNS

Temperature was measured at the indicated time.

250X Electrolytic 10 Per Cent Oxalic Etch RM8461

a. Cold Pressed at 10 Tsi

Note almost complete absence of Cr_2O_3.

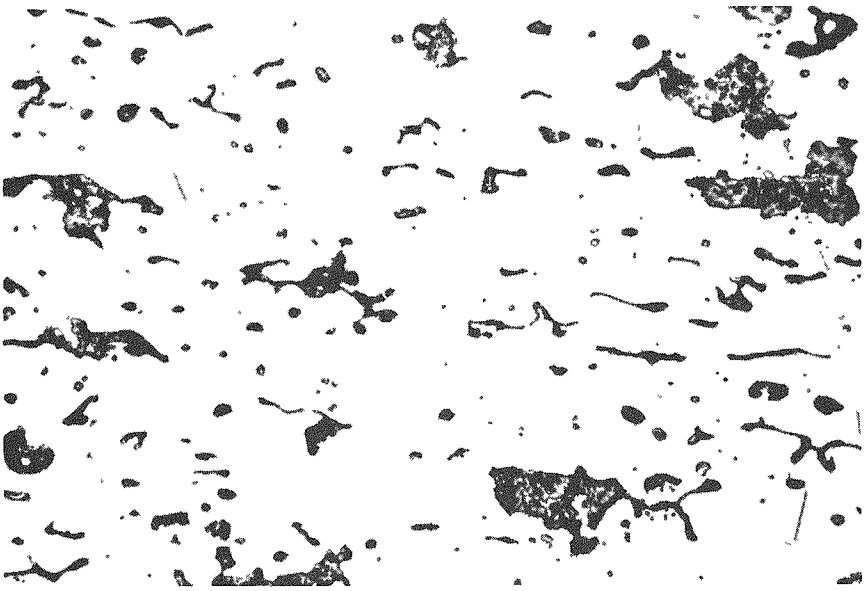

250X Electrolytic 10 Per Cent Oxalic Etch RM8458

b. Cold Pressed at 50 Tsi

Note gray Cr_2O_3 particles.

FIGURE 6. EFFECT OF COMPACTING PRESSURE ON THE REDUCTION OF Cr_2O_3 IN COMPACTS OF 18-14-2.5 ALLOY

Compacts were sintered 48 hr at 2200 F in dry hydrogen and coined at 50 tsi. Porosity is visible in both specimens.

before extensive sintering can occur even when the compact is cold pressed at high pressures. As an example, the worst conditions under which Cr_2O_3-free compacts were produced after cold pressing at 15 tsi consisted of sintering with a maximum dew point of -10 F which recovered to -17 F at 2300 F, while the worst conditions under which Cr_2O_3-free compacts were produced after cold pressing at 35 tsi consisted of sintering with a maximum dew point of -35 F which recovered to -42 F at 2300 F.

TABLE 3. EFFECT OF COMPACTING PRESSURE ON DENSITY AND DEGREE OF Cr_2O_3 REDUCTION IN 18-14-2.5 ALLOY

Compacting Pressure, tsi	Density, per cent of theoretical			Thickness of Cr_2O_3-Free Layer, in.
	Green	Sintered[a]	Coined[b]	
10	60.2	85.6	93.8	0.134
20	66.8	87.5	93.9	0.070
30	73.0	89.0	94.2	0.054
40	78.6	90.6	94.5	0.030
50	82.6	91.0	94.5	0.025

(a) Sintered 48 hr at 2200 F.
(b) Coined at 50 tsi.

The furnace exit dew point is dependent upon both the dryness of the entering hydrogen and the weight of material charged in the furnace. Hydrogen with a -100 F dew point can be readily obtained by passing tank hydrogen through a purification system consisting of (1) a palladium catalyst which converts oxygen to water vapor, (2) an activated-alumina drying tower, and (3) a molecular-sieve (synthetic zeolite produced by Linde Company) drying tower. As oxide is reduced the hydrogen dew point increases, but if only a small amount of water vapor is produced the exit dew point will quickly recover to a low value. Increasing the furnace charge increases the amount of water vapor produced and it may not be possible to obtain a low dew point even when high hydrogen flow rates are used. For a furnace containing a hot zone of 4 in. in diameter by 15 in. long and a hydrogen flow rate of approximately 15 ft^3 per hr, the maximum dew point and the recovery dew point are shown in Table 4 for 25 w/o UO_2-stainless compacts of several weights.

Sintering times and temperatures, although more important from the standpoint of densification, are other factors which affect the reduction of Cr_2O_3. The effect of time can be illustrated by the curves in Figure 7. The rate of densification is very rapid in the first 2 to 4 hr but thereafter long times are required to obtain an appreciable gain in density. The reduction of Cr_2O_3 is also more rapid in the early stages when diffusion of

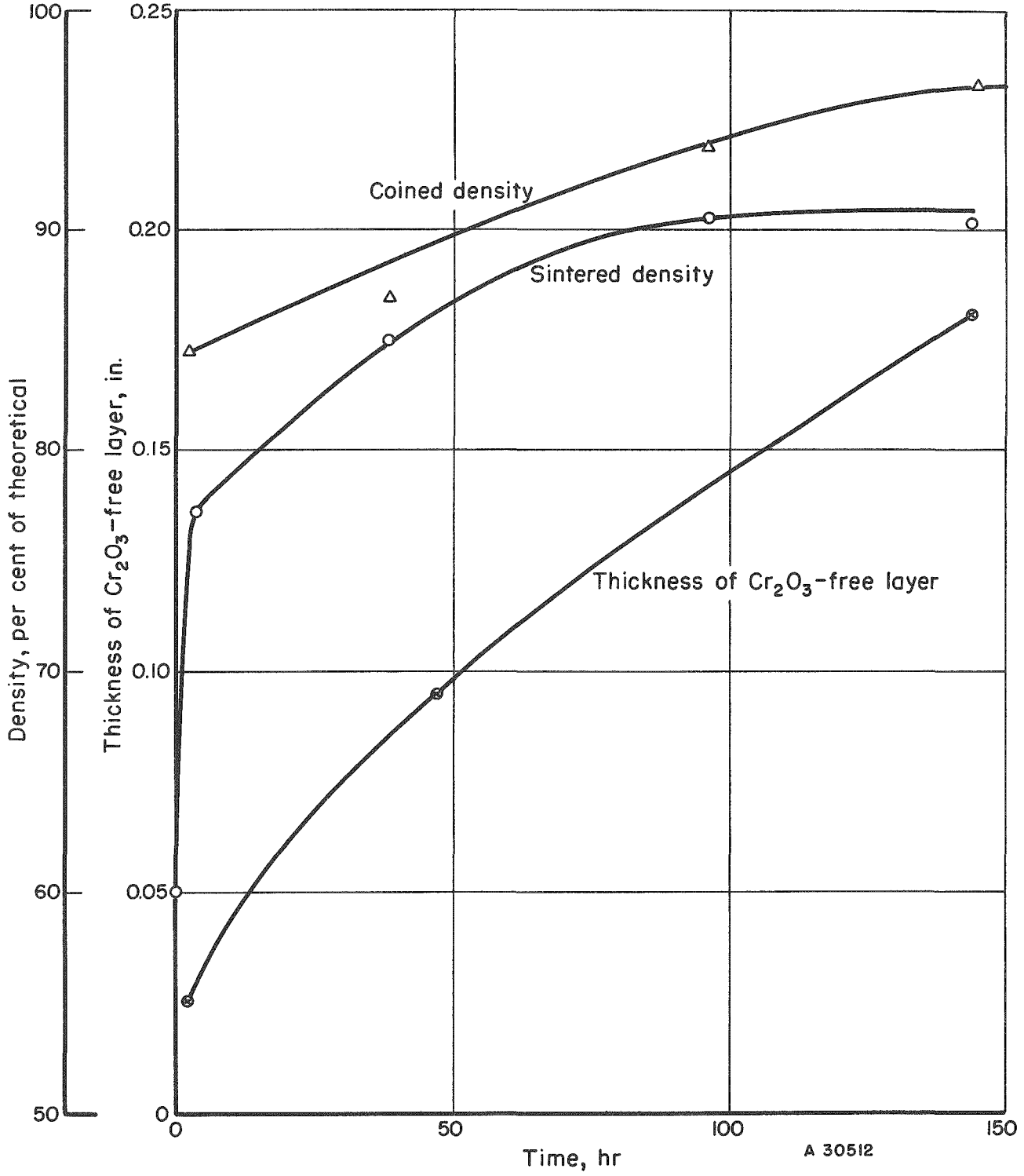

FIGURE 7. EFFECT OF SINTERING TIME AT 2200 F ON DENSITY AND DEGREE OF Cr_2O_3 REDUCTION OF ELEMENTAL 18-14-2.5 ALLOY MIXTURES

the hydrogen and water vapor is more rapid. The results indicate that even though long periods of time are required reduction will continue until all Cr_2O_3 is removed. However, it is possible that as the Cr_2O_3 is reduced a dense surface layer of sintered alloy will be formed and the diffusion of water vapor from the center of the core will be at a low rate. In one series of specimens, for which the data are listed in Table 5, this behavior has occurred.

TABLE 4. EFFECT OF SPECIMEN WEIGHT ON FURNACE EXIT DEW POINT[a]

Total Specimen Weight, g	Maximum Dew Point, F	Recovery Dew Point, F
50	-49	-56
128	-35	-49
252	-16	-29
504	-1	-14

(a) Specimens of 25 w/o UO_2 in an elemental matrix of iron-18 w/o chromium-14 w/o nickel-2.5 w/o molybdenum sintered by a technique described in Appendix A.

The effect of increasing the sintering temperature is more complex. Diffusion is more rapid and densification, homogenization of the alloy, and reduction of the Cr_2O_3 are promoted. However, at temperatures above 2300 F, a ceramic muffle was used and contamination occurred more readily than when a Inconel muffle was used. Also the interconnecting pores near the outside surfaces of the compact apparently were closed before the Cr_2O_3 was completely reduced, and thus, even though a higher dew point can be tolerated at higher temperatures, the data in Table 5 do not indicate that there is a significant reduction of Cr_2O_3 due to an increase in temperature above 2300 F.

The most practical method of reducing the Cr_2O_3 is a step-sintering procedure which allows the use of commerical hydrogen furnaces and commercially available metal powders. The method requires a 1600 F sintering treatment and a slow heating to the maximum sintering temperature. At 1600 F no extensive densification occurred and with low-density compacts, hydrogen flow through the compact was sufficient to reduce most of the iron oxide before it could be converted to Cr_2O_3. The low heating rate allows continuous reduction of the oxides before rapid sintering at high temperatures seals the pores and lowers the rate at which hydrogen diffuses into the specimen and water vapor diffuses out. By pressing at 10 tsi, Cr_2O_3-free compacts were obtained by step sintering to 2200 F, but the green strength of the compacts was poor and a total of 28 hr (18 hr at 1600 F, 6 hr heating to 2200 F, 4 hr at 2200 F) was required. A 2300 F sintering temperature cut the total time required to 18 hr (12 hr at 1600 F, 4 hr heating to 2300 F, 2 hr at 2300 F) and permitted cold compacting at 15 tsi. When annealed iron powder containing 0.25 w/o oxygen was used, the time required was lowered to 10 hr (4 hr at 1600 F, 4 hr heating to 2300 F, 2 hr at 2300 F) for compacts cold pressed up to 30 tsi.

TABLE 5. EFFECT OF SINTERING TIME AND TEMPERATURE ON DENSITY AND DEGREE OF Cr_2O_3 REDUCTION

Nominal Composition (Balance Iron), w/o	Time, hr	Temperature, F	Density[a], per cent of theoretical			Thickness of Cr_2O_3-Free Layer, in.
			Green	Sintered	Coined	
18 Cr-14 Ni-2.5 Mo	2	2200	59.2	77.0	87.0	0.058
	4[b]	2200	57.0	76.4	91.0	0.185 (no Cr_2O_3)[c]
	48	2200	60.2	86.0	93.8	0.122
	96	2200	58.3	89.5	94.3	0.148
	144	2200	58.5	89.4	96.5	0.129
18 Cr-9 Ni	2	2200	59.7	77.6	84.5	0.027
	4[b]	2200	57.4	75.7	87.5	0.140[c]
	48	2200	59.8	84.9	86.8	0.096
	96	2200	58.3	90.8	93.4	--
	144	2200	57.8	90.4	96.6	0.187 (no Cr_2O_3)
18 Cr-14 Ni-2.5 Mo	2	2300	61.0	80.2	88.9	0.074
	2	2400	60.0	82.6	91.7	0.067
18 Cr-8 Ni	2	2300	59.5	77.7	87.6	0.067
	2	2400	58.7	81.6	90.0	0.057

(a) Green compacting pressure of 10 tsi and coining pressure of 50 tsi.
(b) Specimen sintered by holding 18 hr at 1600 F and heating at 100 F per hr to 2200 F and holding at temperature for 4 hr.
(c) Thickness cannot be compared directly with other specimens since a step-sintering technique was used.

If it is desired to obtain a homogeneous sintered alloy, long sintering times are required. Times on the order of 150 hr at 2200 F, or 60 to 70 hr at 2300 F are necessary for placing all the chromium in solution. This process is not readily adaptable to quantity production of fuel elements. However, as discussed in a later section, it is possible to dissolve the chromium at a much higher rate by heat treating after hot roll cladding. Therefore, it is desirable to use the step-sintering technique even though the presence of free chromium and chromium-rich ferrite may be detected in the as-sintered specimens. Other than the removal of the Cr_2O_3 film surrounding the chromium particles and the use of a relatively high sintering temperature (2300 F), the control of chromium powder particle size is the most important factor in the dissolution of chromium. As shown in Figure 8, the most favorable results are obtained with minus 400-mesh chromium powder, but satisfactory results are obtained with minus 325-mesh powder.

As shown in Table 6, additions of UO_2 have some effect on densification. Previous work[1] has shown that a pronounced increase in porosity occurs when small UO_2 particles (1 to 5 μ) are added, but the increase is not great when large UO_2 particles are used. The data do indicate, however, that there is a tendency for density to decrease with decreasing UO_2 particle size and increasing loading.

Prealloyed Stainless Steel

Because of the tendency for green prealloyed compacts to break up when handled, only compacts pressed at 30 tsi or higher were used. Most of the specimens contained 25 w/o UO_2 and very little work was done with unfueled compacts. Information on sintered compact densities, mechanical properties, and microstructures has been reported by Grobe and Roberts[3] for Types 302B, 316, 318, 318 Si, and 431 stainless prealloyed powders.

Prealloyed powders were sintered in hydrogen atmospheres by the simple procedure of loading compacts directly into the hot zone at the sintering temperature, holding at temperature for 2 to 4 hr, and cooling rapidly in the furnace cold zone.

One of the major advantages usually cited for prealloyed powder is the homogeneous structure which can be obtained without extensive diffusion. However, an examination of the chemical composition of Type 318 prealloyed powder shows a high silicon content, and it would be expected that during the sintering operation, the silicon would promote the formation of ferrite, particularly if the carbon content is reduced with the hydrogen atmosphere. The high silicon content is usually desirable because of the increased moldability and green strength of the powders as compared with powders with little or no silicon. If a low-silicon-bearing powder is used, the formation of ferrite can be prevented but, due to oxygen contamination during the shotting process, the specimens will contain chromium-rich chromium-iron oxides, as shown in Figure 9. Even when complex sintering techniques are used, it is difficult to completely reduce these oxides. As illustrated in Figure 10, the step-sintering procedure developed for reducing Cr_2O_3 in elemental stainless steel matrices did not result in complete reduction of the Cr_2O_3

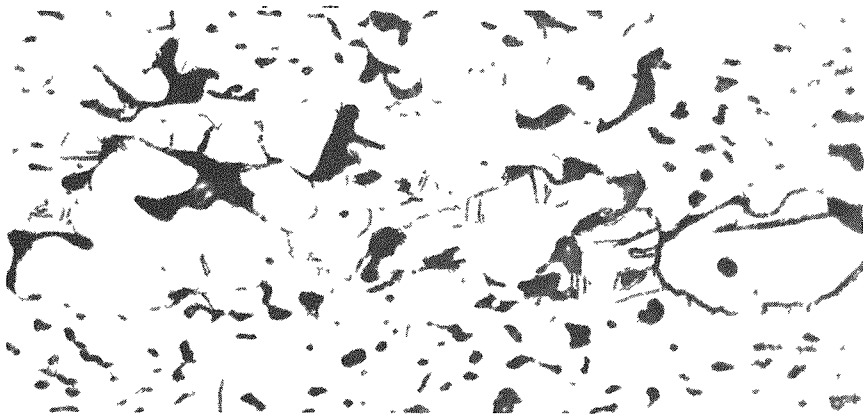

250X 10 Per Cent Oxalic Etch RM11407

a. Minus 200 Plus 325-Mesh Electrolytic Chromium Powder

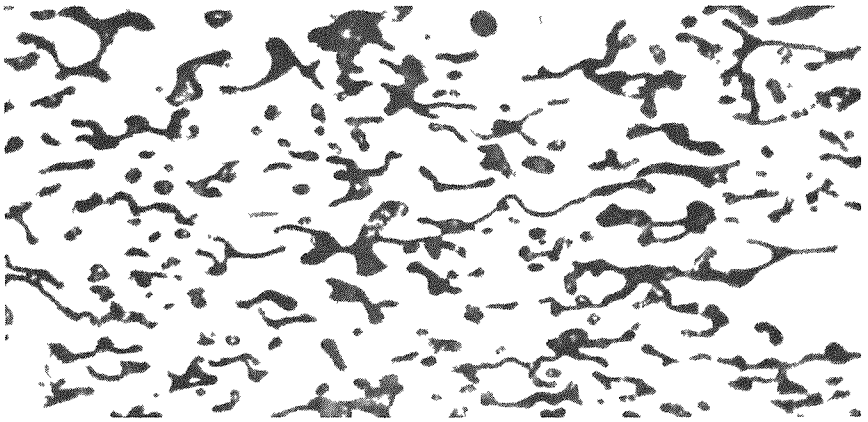

250X 10 Per Cent Oxalic Etch RM11408

b. Minus 325-Mesh Electrolytic Chromium Powder

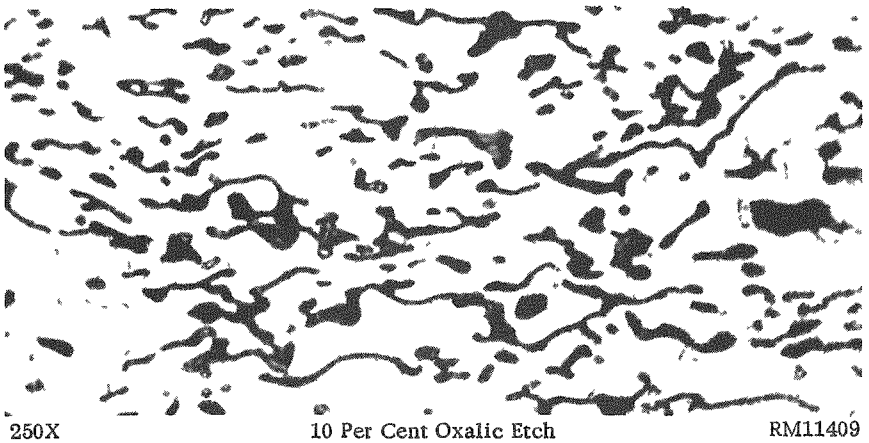

250X 10 Per Cent Oxalic Etch RM11409

c. Minus 400-Mesh Electrolytic Chromium Powder

FIGURE 8. EFFECT OF CHROMIUM PARTICLE SIZE ON THE STRUCTURE OF 18-14-2.5 ALLOYS STEP SINTERED TO 2300 F

Note that chromium dissolution increases with decreases in particle size.

TABLE 6. EFFECT OF UO_2 LOADING AND PARTICLE SIZE ON SINTERABILITY OF 18-14-2.5 ALLOY

UO_2, w/o	UO_2 Particle Size, μ	Density, per cent of theoretical		
		Green	Sintered[a]	Coined[b]
--	--	65.7[c]	77.9	89.7
15	<44	63.8[c]	72.5	86.0
25	<44	64.5[c]	70.3	85.3
35	<44	66.0[c]	69.3	83.0
15	74-149	64.5[c]	75.2	86.0
20	74-149	65.1[c]	73.5	85.9
30	74-149	66.2[c]	72.4	85.0
35	74-149	65.0[c]	71.6	83.8
25	105-149	81.6[d]	83.6	89.2
25	74-149	82.2[d]	84.0	89.1
25	53-74	80.5[d]	81.7	88.4
25	44-53	81.8[d]	82.1	88.3

(a) Step sintered to 2300 F by process described in Appendix A.
(b) Coined at 50 tsi.
(c) Compacted at 15 tsi.
(d) Compacted at 50 tsi.

500X As Polished N51830

FIGURE 9. CHROMITE IN LOW-SILICON PREALLOYED TYPE 318 STAINLESS STEEL DUE TO OXYGEN CONTAMINATION OF THE POWDER DURING THE SHOTTING PROCESS

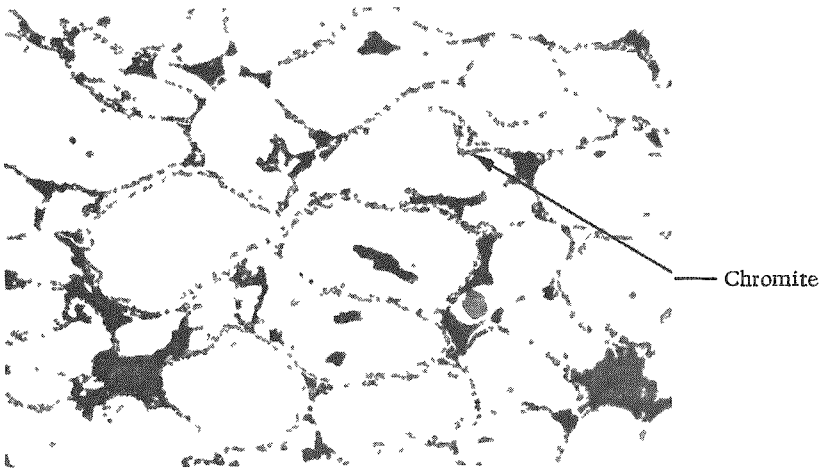

250X As Polished RM11176

FIGURE 10. CHROMITE IN LOW-SILICON PREALLOYED TYPE 318 STAINLESS STEEL SPECIMEN STEP SINTERED TO 2300 F

The step-sintering procedure developed for reducing Cr_2O_3 in elemental stainless matrices did not result in complete reduction of the Cr_2O_3 contained in the low-silicon prealloyed powder.

contained in the low-silicon prealloyed powder. Nevertheless, since the disadvantage of using stainless steels which contain small amounts of a secondary phase has not been clearly demonstrated, the use of the prealloyed powder was not eliminated on this basis.

Sintering studies were directed toward the production of compacts with a maximum of 15 per cent porosity and with a minimum of secondary phases. Sintering temperatures as low as 2100 F were considered as a means of decreasing the decarburization. However, since ferrite could still be detected, as shown in Figure 11, and since double sintering was required to obtain the minimum density, no distinct benefit was gained by sintering at 2100 F. At 2300 F large amounts of large ferrite grains were formed, while at 2200 F the ferrite was usually present as smaller precipitates, but the actual amount varied from 5 to 20 volume per cent. Photomicrographs which show the presence of ferrite are presented in Figure 11. In addition to selective etches, a colloidal suspension of Fe_3O_4 was placed on the specimen and a magnetic field applied for identification of ferritic areas. Confirmation of results was obtained by X-ray diffraction. The low-silicon Type 318 stainless steel may contain 10 to 15 volume per cent chromite after fabrication, as shown in Figure 9. Thus, the percentage of nonmetallic particles may be increased from the 19 volume per cent due to UO_2 to a total of approximately 30 volume per cent.

For the prealloyed powders, no change in composition of individual particles occurs during sintering; therefore, it is not necessary to select a particle size which promotes diffusion of the atoms beyond the distance necessary to obtain a dense compact. However, as shown in Table 7, the particle size may have some effect on the sintered density, but special blends did not greatly improve the sinterability over that of the as-received minus 100-mesh powder. Screen analyses of as-received powders are listed in Table 8.

Data listed in Table 9 show that UO_2 of the particle sizes tested did not greatly affect the sinterability of prealloyed powders. There appeared to be a slight tendency for increased UO_2 loading and decreased UO_2 particle sizes to decrease the density, but the variation in density was within normal limits of compacts produced under similar conditions.

ROLL-CLADDING STUDIES

Long, thin plates of UO_2-stainless steel dispersions clad with stainless steel can be more readily produced by roll-cladding procedures than by other commonly used fabrication methods. Roll cladding offers advantages other than ease of fabrication such as increasing the core density, improving homogeneity of the core, and decreasing fuel segregation. However, several disadvantages inherent in the process tend to produce stringered and fractured UO_2 particles. Variations in hot rolling, cold rolling, and heat treatment can be made to improve the appearance of the UO_2 dispersion, but other factors such as core-to-cladding bond strength, metal grain size, and surface finish must also be considered. Thus, optimum procedures for roll cladding will not necessarily produce the best possible UO_2 dispersion.

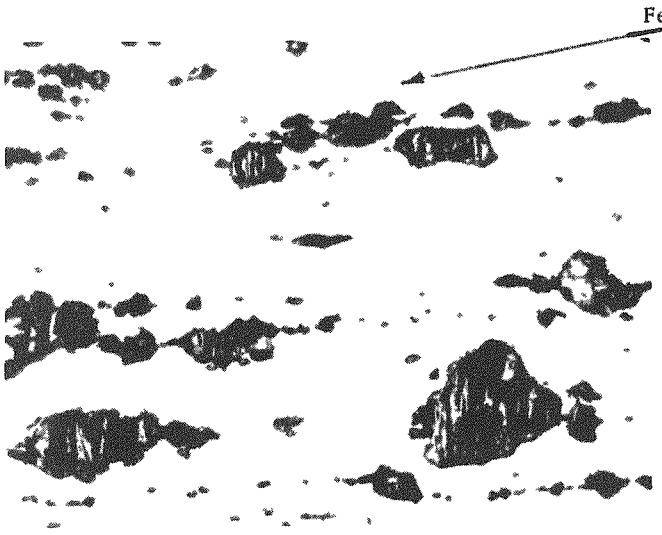

250X Glyceria Regia Etch N53886

a. 25 w/o UO_2 in Type 318 Stainless Sintered 3 Hr at 2100 F and annealed at 2050 F.

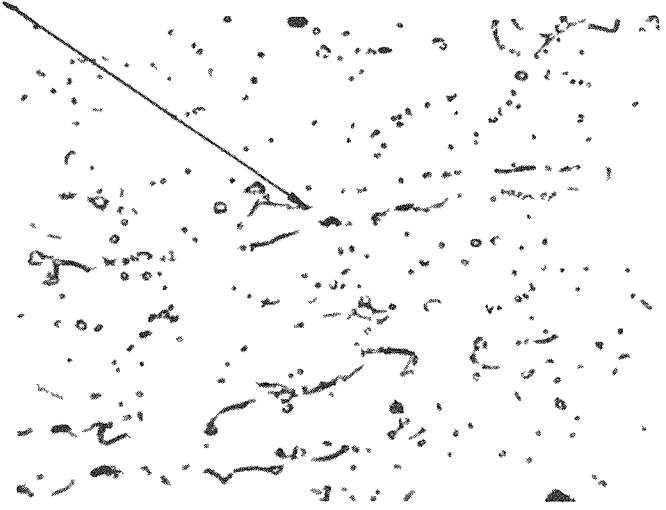

1000X Glyceria Regia Etch N44912

b. 25 w/o UO_2 in Type 318 Stainless Sintered 4 Hr at 2200 F and annealed at 1900 F.

No UO_2 visible.

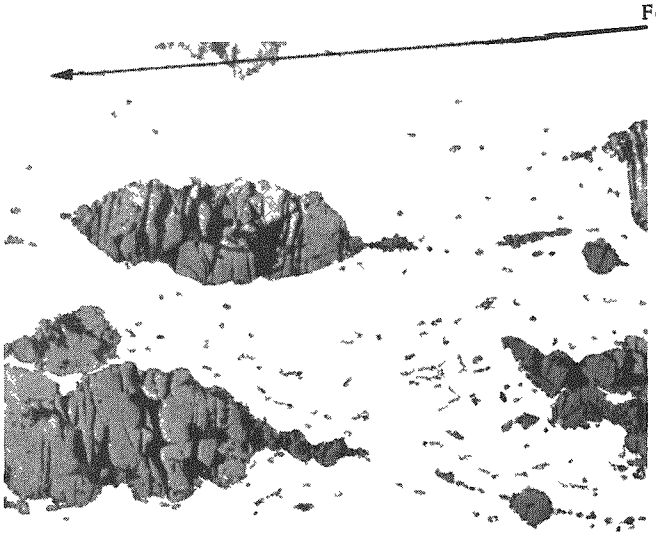

250X Glyceria Regia Etch RM10155

c. 25 w/o UO_2 in Type 318 Stainless Sintered 2 Hr at 2300 F and annealed at 2050 F.

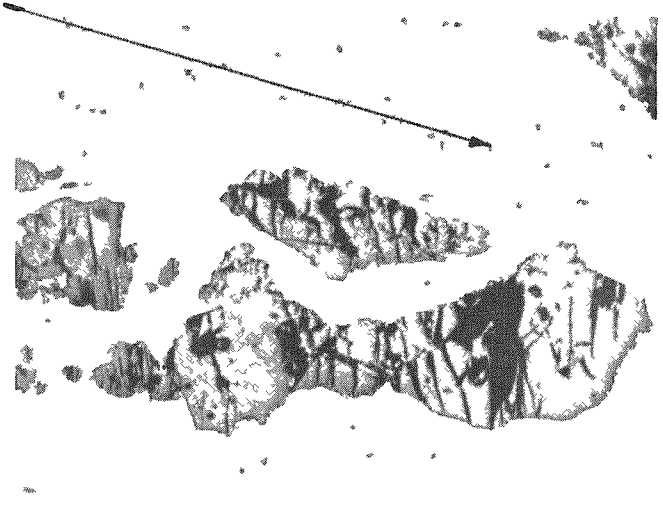

250X Glyceria Regia Etch RM10157

d. 25 w/o UO_2 in Type 302B Stainless Sintered 2 Hr at and annealed at 2050 F.

FIGURE 11. PRESENCE OF FERRITE IN UO_2-STAINLESS STEEL DISPERSIONS

All specimens were hot rolled at 2200 F and cold rolled. White secondary phase is ferrite.

TABLE 7. EFFECT OF METAL POWDER SIZE ON THE SINTERABILITY OF UO_2-TYPE 318 PREALLOYED STAINLESS STEEL COMPACTS

UO_2, w/o	Powder Particle Size, μ		Density, per cent of theoretical		
	UO_2	Type 318	Green[a]	Sintered	Coined[b]
25	74-105	As received, <149	75.3	76.9[c]	84.0
25	74-105	10 w/o <44, 10 w/o 44-53, 80 w/o 105-149	76.5	77.4[c]	84.0
25	74-105	20 w/o <44, 80 w/o 105-149	76.6	79.0[c]	84.5
25	74-105	80 w/o <44, 20 w/o 105-149	73.3	76.8[c]	83.0
20	53-74	As received, <149	77.5	81.3[d]	86.8
20	53-74	80 w/o <44, 20 w/o 105-149	72.6	75.0[d]	81.8
25	74-105	37-44	73.9	79.7[e]	84.4
25	74-105	<37	71.0	80.0[e]	84.4

(a) Compacted at 50 tsi.
(b) Coined at 50 tsi.
(c) Sintered at 2100 F.
(d) Sintered at 2200 F.
(e) Sintered at 2300 F.

TABLE 8. SCREEN ANALYSIS OF PREALLOYED STAINLESS STEEL POWDERS

Mesh Size	Distribution in Indicated Metal Powder, w/o			
	302B	347	318	318 Si
+100	--	0.6	0.3	0.5
-100+140	--	19.1	18.4	11.7
-140+200	3.5	22.0	24.8	22.9
-200+325	55.8	40.1	27.5	31.2
-325	40.7	18.2	29.0	33.7

TABLE 9. EFFECT OF UO_2 LOADING AND PARTICLE SIZE ON SINTERABILITY OF TYPE 318 PREALLOYED STAINLESS STEEL POWDERS

UO_2, w/o	Powder Particle Size, μ		Density, per cent of theoretical		
	UO_2	Type 318	Green[a]	Sintered[b]	Coined[c]
15	<44	53-75	80.1	80.5	87.8
25	<44	53-75	80.4	81.0	87.2
35	<44	53-75	80.4	81.0	86.0
20	74-149	53-75	79.4	80.5	86.3
30	74-149	53-75	80.4	81.0	86.5
35	74-149	53-75	80.0	80.5	86.7
0	--	<149	77.0	77.8	87.3
20	105-149	<149	77.4	82.5	86.8
20	74-105	<149	77.7	81.4	86.8
20	53-74	<149	77.5	81.3	86.8
20	44-53	<149	78.6	81.0	88.2

(a) Compacted at 50 tsi.
(b) Sintered at 2200 F for 4 hr.
(c) Coined at 50 tsi.

Hot Rolling

The hot-rolling operation serves the purposes of creating a metallurgically sound core-to-cladding bond, densifying the core, and extending the plate to very near its final length. Factors which have been considered include picture-frame pack design, furnace atmospheres, rolling temperatures, rates of reduction, and total reduction.

Components of a picture-frame pack of the type used in this study are shown in Figure 12. In production it would probably be more desirable to use a one-piece frame with a small radius at each inside corner, but because of frequent changes in core dimensions, experimental work can be conducted faster and cheaper with square-corner split dies and square-corner two-piece picture frames. The interlocking design assures a metallurgical bond between the two frame components, as shown by the radiograph and photomicrograph in Figure 13. It was considered necessary to use an evacuated pack since development studies were made for plates to be used at temperatures on the order of 1500 F and core-to-cladding bonds of the highest integrity were required. Good core-to-cladding bonds can be produced without evacuated packs, but failures frequently occur and a blister anneal or nondestructive tests must be depended upon to locate plates with defects, and, thus far, no test is being applied to UO_2-stainless plates which can detect small defects. In this investigation over 400 plates were fabricated in evacuated packs. More than 50 of these plates were subjected to metallographic examination along the full length of the core and an additional 150 to 200 plates were examined in random locations. In no case was a defective core-to-cladding bond detected. Blisters did occur in four plates. Of these, welds broke on the first rolling pass in two cases and an evacuation stem broke on one pack during the first pass. Metallographic examination indicated the failure of the fourth pack may have been due to improper cleaning of the components before welding. In order to remove all entrapped gases packs were evacuated at 500 to 600 F and the stems were forged closed.

When rolling temperatures on the order of 2200 F were used it was necessary to control the furnace atmosphere in order to prevent excessive scaling of the stainless steel. Figure 14 shows the effect of rolling from air, hydrogen, and argon atmospheres. Forming gas was also tested, but results were poorer than obtained with argon. The hydrogen atmosphere resulted in the formation of a thin adherent oxide film which could be easily removed after hot rolling by pickling in a warm solution of 5 parts HF, 15 parts HNO_3, and 80 parts water for 5 min. It was not necessary to dry or otherwise purify tank hydrogen for the rolling; however, a flash-back arrester was placed in the line between the furnace and hydrogen tank.

Rolling temperatures in the range 1900 to 2200 F were investigated. Good core-to-cladding bonds can be achieved at any temperature in this range but core structures vary with the temperature. As shown in Figure 15, the individual UO_2 particles are more severely broken up and stringered and fewer particles are completely surrounded by matrix metal in plates rolled at 1900 F than in plates at 2200 F. For comparison of the microstructures shown, the fine, dark, stringered precipitate which was identified as Cr_2O_3 should not be considered. Since the specimens were sintered at 2200 F, all of the Cr_2O_3 was not reduced. As shown in Figure 16, similar results are obtained with prealloyed powders but a more severe fracturing of UO_2 occurs at all temperatures. The

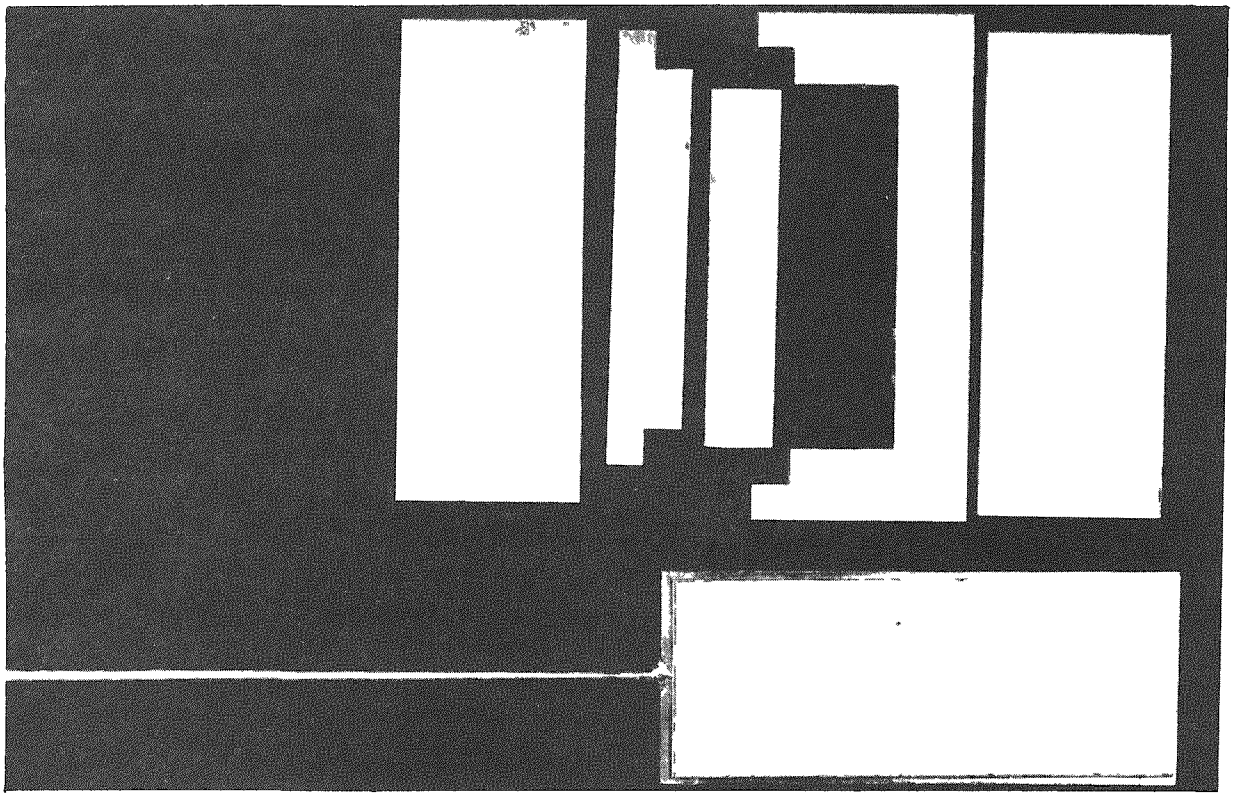

1/2X RM9344

FIGURE 12. COMPONENTS OF A STAINLESS STEEL PICTURE-FRAME PACK

F512

a. Positive Print of Radiograph

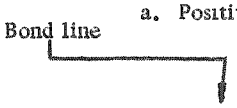

250X RM11418

b. Structure of Interface Parallel With Rolling Direction

FIGURE 13. METALLURGICAL BOND OBTAINED WITH TWO-PIECE INTERLOCKING PICTURE FRAME AFTER ROLLING

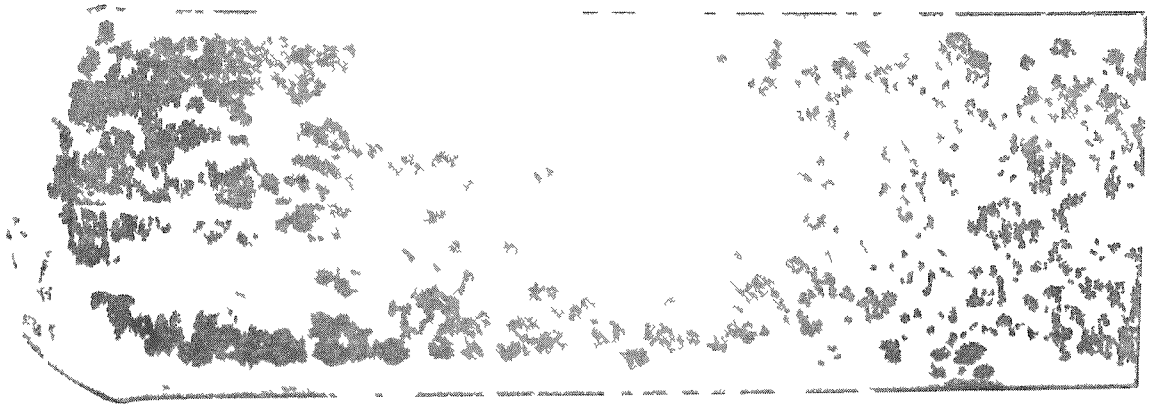

RM11400

a. Rolled in Air (Appearance Before Pickling)

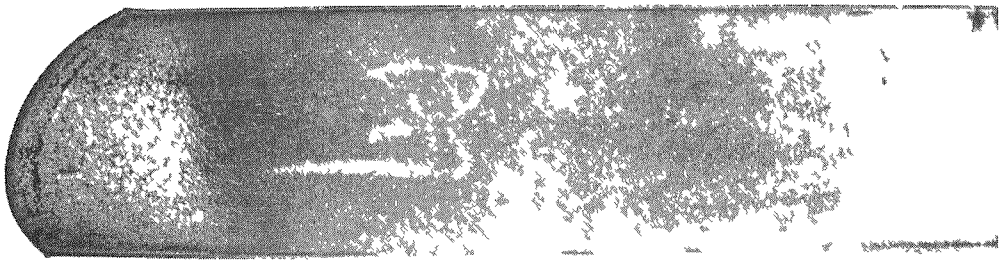

RM11402

b. Rolled in Argon (Appearance Before Pickling)

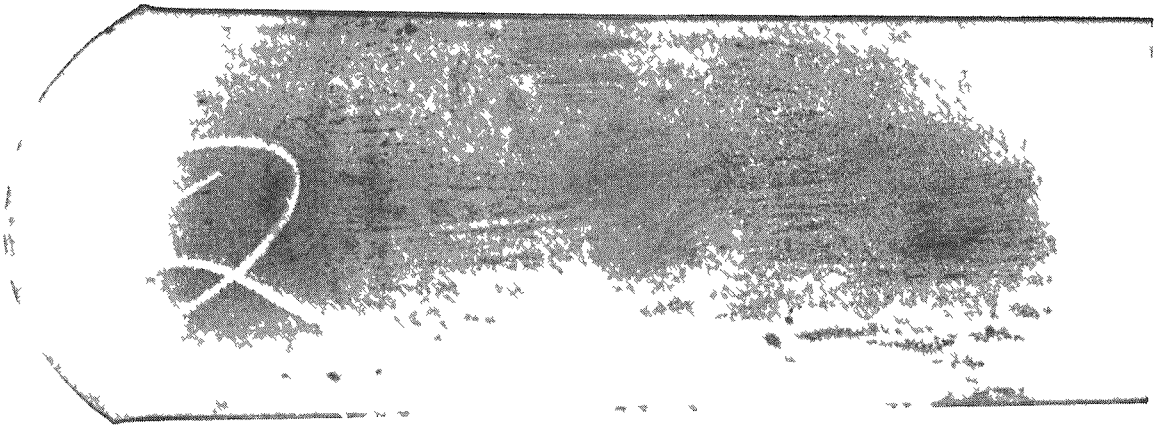

RM11401

c. Rolled in Hydrogen (Appearance Before Pickling)

FIGURE 14. OXIDE SCALE AND PICKLED SURFACE OF TYPE 318 STAINLESS ROLLED AT 2200 F IN ATMOSPHERES OF AIR, ARGON, AND HYDROGEN

As can be seen in the photographs, best results were obtained with the hydrogen atmosphere; the thin oxide layer was easily removed by pickling.

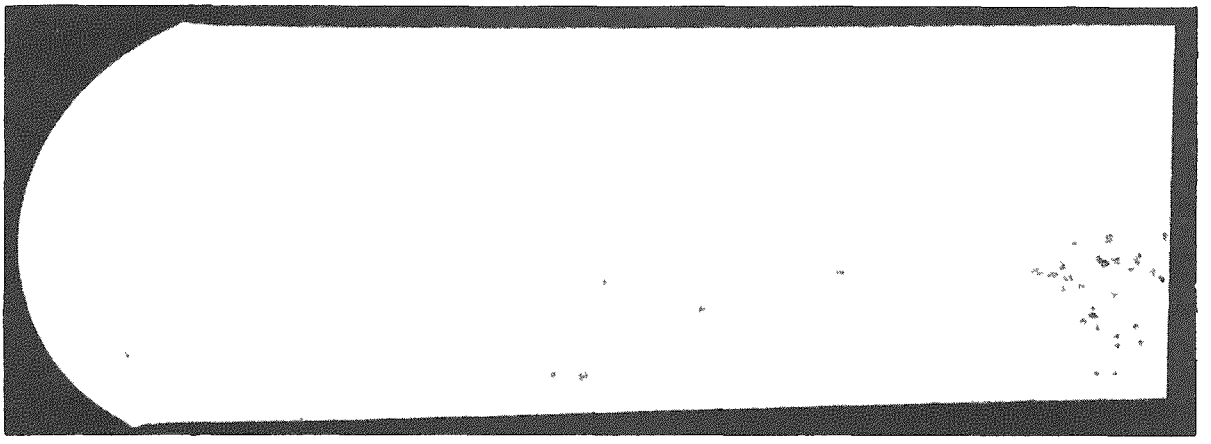

RM11403

a. Rolled in Air (Appearance After Pickling)

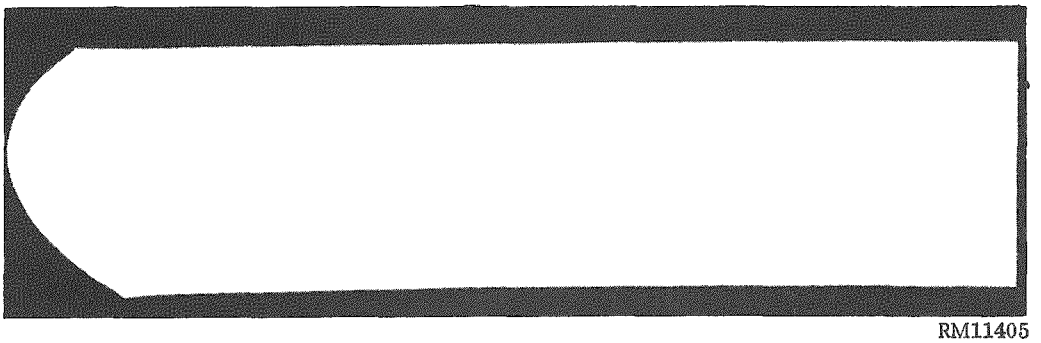

RM11405

b. Rolled in Argon (Appearance After Pickling)

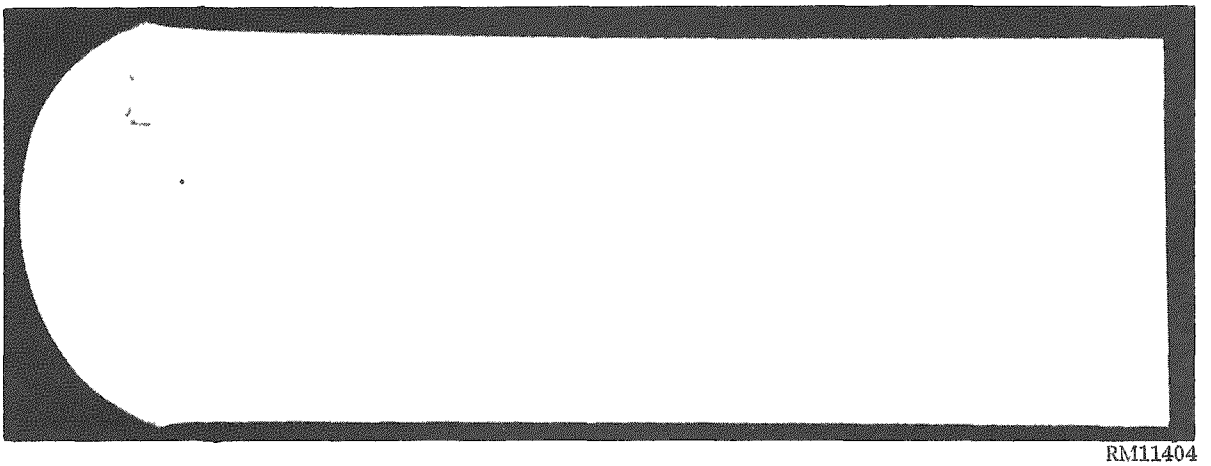

RM11404

c. Rolled in Hydrogen (Appearance After Pickling)

FIGURE 14. (Continued)

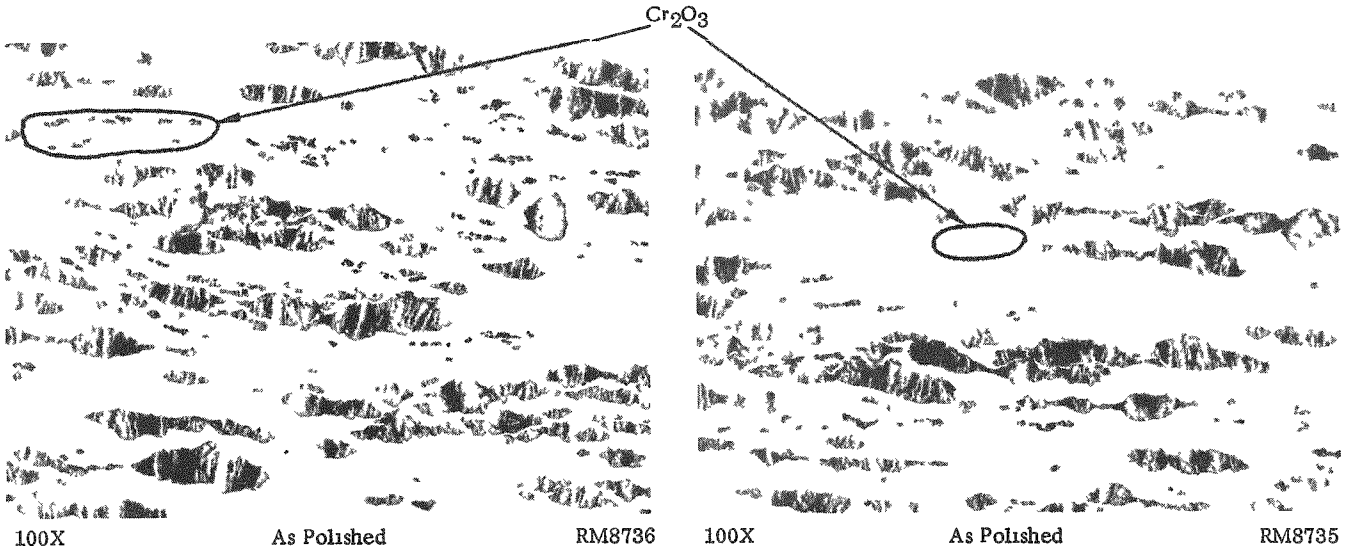

a. Hot Rolled at 1900 F

b. Hot Rolled at 2000 F

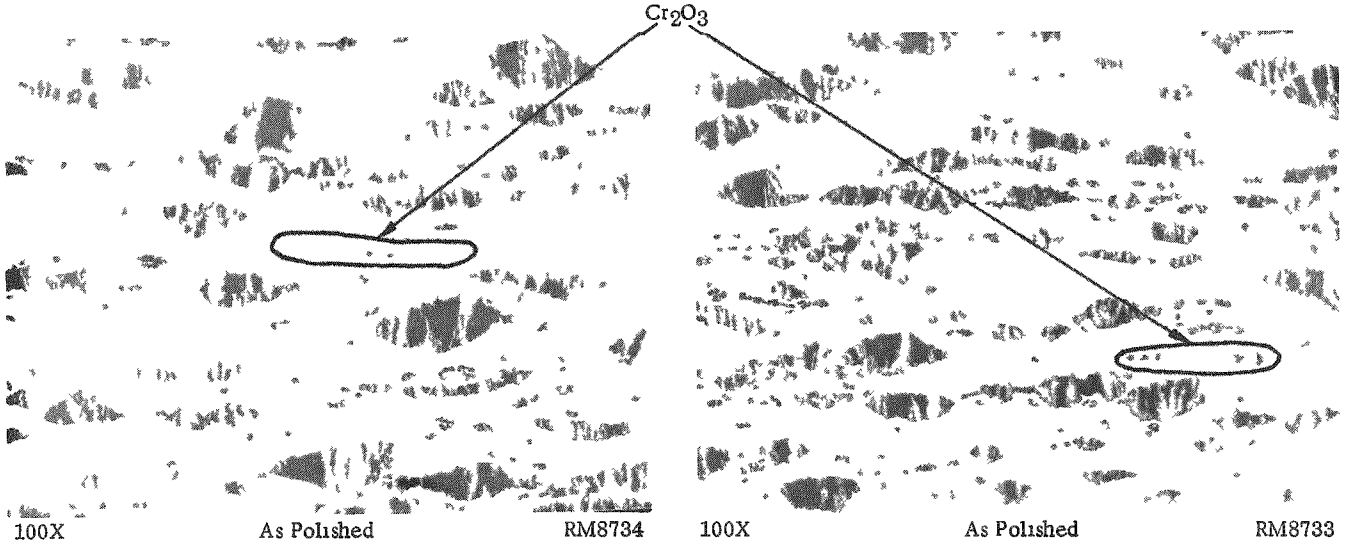

c. Hot Rolled at 2100 F

d. Hot Rolled at 2200 F

FIGURE 15. EFFECT OF HOT-ROLLING TEMPERATURE ON THE FRACTURING AND STRINGERING OF UO_2 PARTICLES IN AN 18-14-2.5 ALLOY MATRIX

At the lower rolling temperature, the individual UO_2 particles are more severely broken up and stringered and fewer particles are completely surrounded by matrix metal. Since all of the specimens were sintered at 2200 F, all of the Cr_2O_3, evident in the microstructures as a fine, dark, stringered precipitate, was not reduced and should not be considered when comparing the microstructures. Voids in UO_2 particles are due to metallographic pull-out Specimens were sintered at 2200 F and hot roll clad to a reduction of 6 to 1 in thickness, annealed for 2 hr at 2000 F, and cold reduced 20 per cent in thickness.

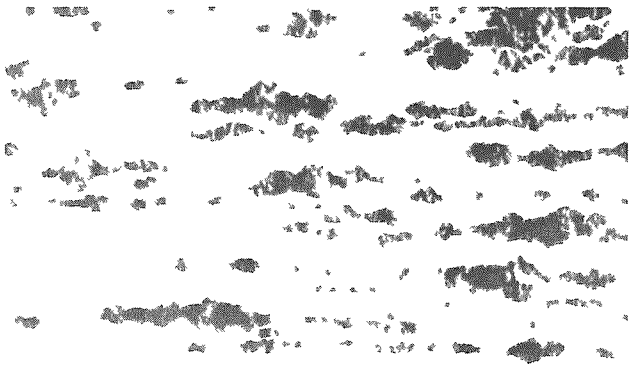

100X As Polished RM8919

a. Hot Rolled at 1900 F

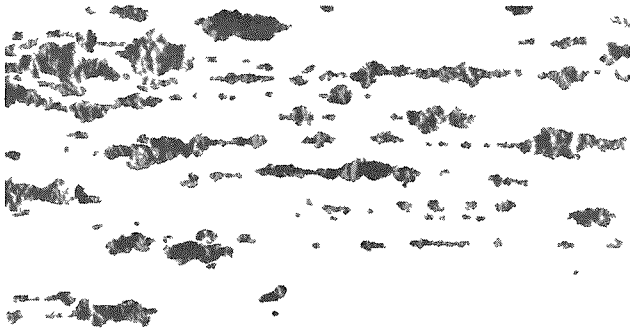

100X As Polished RM8920

b. Hot Rolled at 2000 F

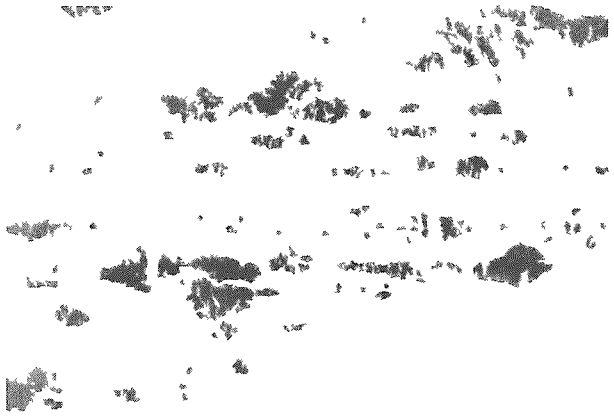

100X As Polished RM8921

c. Hot Rolled at 2100 F

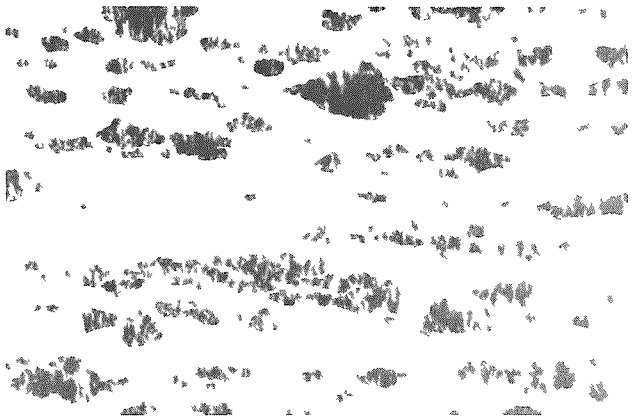

100X As Polished RM8922

d. Hot Rolled at 2200 F

FIGURE 16. EFFECT OF HOT-ROLLING TEMPERATURE ON THE FRACTURING AND STRINGERING OF UO_2 PARTICLES IN A PREALLOYED TYPE 318 STAINLESS STEEL MATRIX

Note that more severe fracturing of UO_2 occurs with prealloyed powders than with elemental powders (Figure 15). Specimens were sintered at 2200 F, hot roll clad to a reduction of 6 to 1 in thickness, annealed 2 hr at 2000 F, and cold rolled to a 20 per cent reduction in thickness.

temperatures discussed above are furnace temperatures. The actual temperature of the plate dropped approximately 200 F as it passed through the rolls. The temperature of the plate after passing through the rolls was approximately 350 F lower.

The rate of reduction used on the first pass can be related to the final core structure and the first pass is probably the most important pass as far as achieving a good core-to-cladding bond is concerned. Good core-to-cladding bonds are obtained for a wide range of initial reduction rates. Previous work[1] has indicated that if an initial reduction in thickness of 10 per cent is used there is a greater tendency for stringering of UO_2 particles and the core-to-cladding bond is not as good as when initial reductions of 25 to 50 per cent in thickness are used. As shown in Figure 17, the effect on microstructure is not great, but it appears to be beneficial to use higher initial rates of reduction. Although good structures were obtained when a 50 per cent reduction in thickness was used on the first pass, no improvement in structure was obtained by using a higher reduction rate than 40 per cent in thickness on the first pass. Satisfactory results were obtained when a 20 per cent reduction in thickness was used for all remaining passes. No significant improvement was noted when a 10 per cent reduction in thickness per pass was used after the initial pass.

An increase in total reduction tends to increase fracturing and stringering of UO_2 particles. However, in the range considered (5 to 1 to 8 to 1 total reduction in thickness) the effect was small, but even in the most severe case the final core thickness was five times the original diameter of the largest UO_2 particle used.

After annealing at the rolling temperature for 1 hr, fine equiaxed grains were obtained in both prealloyed and elemental core matrices. In the elemental matrices stringers of chromium-rich areas could be detected, while from 5 to 20 volume per cent of ferrite could be seen in the prealloyed matrices. The cladding material consisted of larger fully annealed grains containing coarse niobium carbide-nitride complex particles as well as the fine NbC precipitate. Additional discussion of the rolled structure is included in the section on heat treating.

Cold Rolling

Close tolerances placed on fuel-element thickness, straightness of core, and surface finish can be met only when a cold-rolling operation is included in the fabrication process. However, cold rolling can also cause severe fracturing and stringering of UO_2 particles. Variations in sintering incurred during hot rolling can be completely ignored if cold reduction is large.

The effect of cold work on the appearance of the UO_2 dispersion is illustrated in Figure 18. Cold work also tends to decrease core densities slightly as shown in Table 10. In addition, mechanical strength decreases as a result of the change in structure. The room-temperature tensile strength of the specimens shown in Figure 18 (measured in the thickness direction) decreased from 13,800 psi for the 14.3 per cent cold-worked specimen to 8,600 psi for the 69 per cent cold-worked specimen.

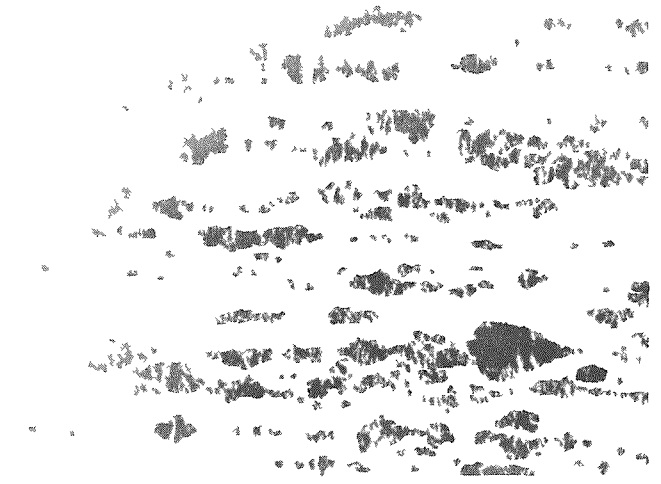

100X As Polished RM8922

a. 30 Per Cent First Pass

25 w/o UO_2 in prealloyed Type 318 matrix; minus 140 plus 200-mesh UO_2.

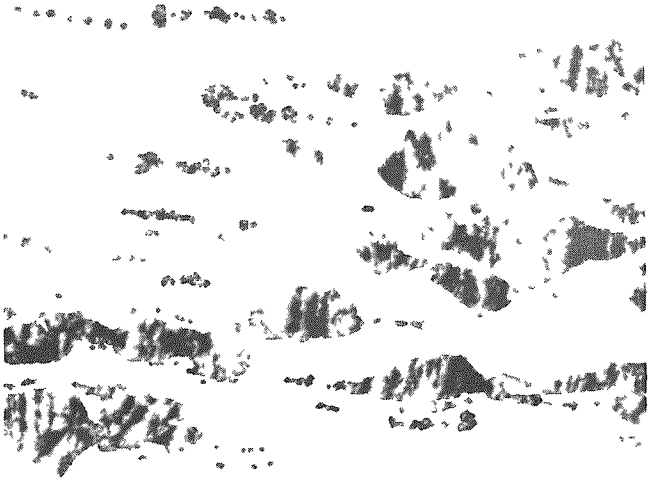

100X As Polished RM8319

b. 30 Per Cent First Pass

25 w/o UO_2 in 18-14-2.5 elemental matrix minus 100 plus 140-mesh UO_2.

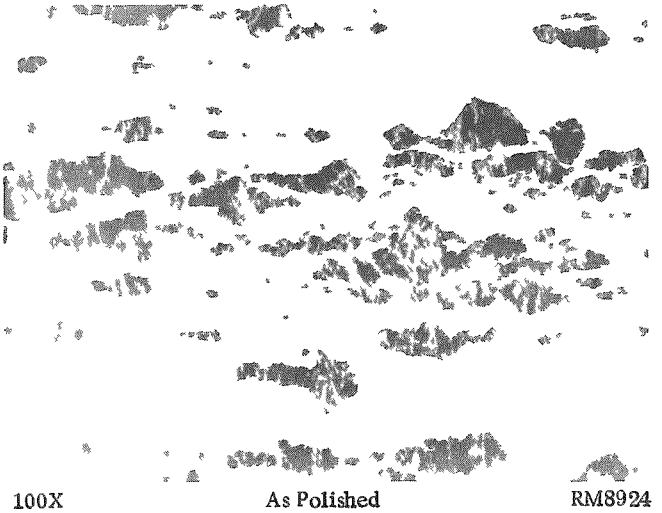

100X As Polished RM8924

c. 40 Per Cent First Pass

25 w/o UO_2 in prealloyed Type 318 matrix; minus 140 plus 200-mesh UO_2.

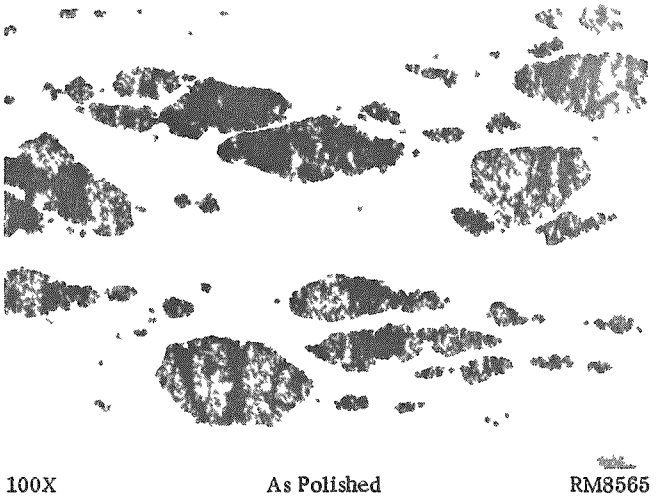

100X As Polished RM8565

d. 40 Per Cent First Pass

25 w/o UO_2 in 18-14-2.5 elemental matrix; minus 100 plus 140-mesh UO_2.

FIGURE 17. EFFECT OF INITIAL RATE OF REDUCTION ON FINAL CORE STRUCTURE

A slight improvement in microstructure is evident in the specimens given the heavier initial reduction.

100X As Polished RM8317

a. Before Cold Rolling

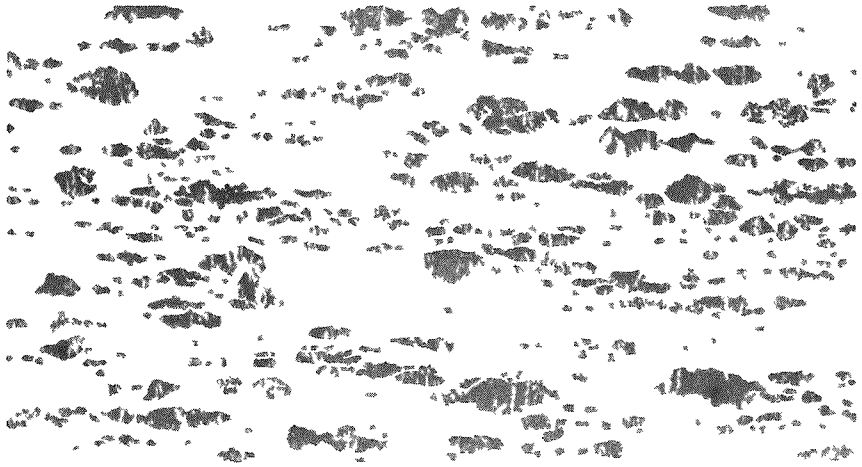

100X As Polished RM8325

b. After 14.3 Per Cent Reduction in Thickness

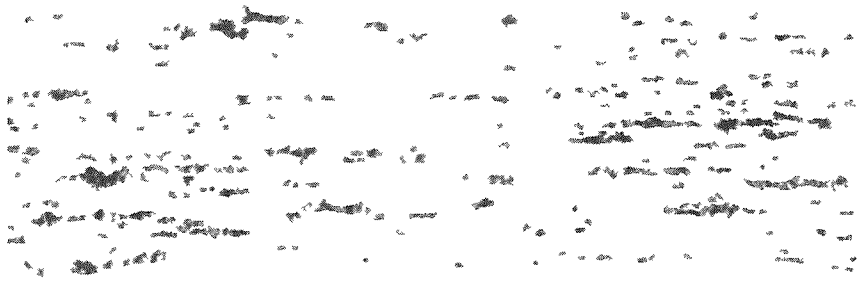

100X As Polished RM8318

c. After 69 Per Cent Reduction in Thickness

FIGURE 18. DELETERIOUS EFFECTS OF COLD ROLLING TO HEAVY REDUCTIONS ON FINAL CORE STRUCTURE

25 w/o UO_2 (minus 270 plus 325-mesh size) dispersed in 18-14-2.5 elemental matrix, sintered at 2200 F, roll clad at 2200 F, annealed at 2000 F, and cold rolled.

TABLE 10. EFFECT OF COLD WORK ON DENSITY OF ROLL-CLAD 25 w/o UO_2 ELEMENTAL 18-14-2.5 MATRICES

Cold Reduction, per cent	Specimen[a] Density, g per cm^3	Calculated Core Density, g per cm^3	Density of Core, per cent of theoretical
0	8.15	8.27	97.5
10	8.08	8.16	96.2
30	8.01	8.07	95.1
50	8.05	8.13	95.8

(a) Measured on same specimen by immersion. Both water and CCl_4 were used. Specimen includes 30 volume per cent wrought stainless steel cladding.

The use of light reductions (approximately 1 per cent per pass) in thickness were found to be beneficial in reducing the detrimental effect on the UO_2. It was also found to be desirable to anneal after the final hot-rolling pass in order to remove any residual stresses before cold rolling. Approximately 14 per cent cold work was necessary to obtain pit-free surfaces.

Heat Treating

Both the microstructures and mechanical properties of the fuel elements are controlled to a certain extent by heat treatments given during and after roll cladding. Since the fuel element was designed for service at approximately 1500 F, it was desired to produce a corrosion-resistant alloy with a minimum of ferrite, sigma, and oxides, and with good mechanical strength at 1500 F. Also, bending around at least a 4.2T bend was required for room-temperature fabrication of subassemblies.

Corrosion resistance is partially dependent upon the absence of chromium carbide or chromium-depleted areas. Detailed discussions on carbides and the stabilization of stainless steels have appeared in the open literature.[4,5,6] A final anneal at 2050 F gives satisfactory results. Since the fuel-element service temperature lies within the critical range of 1000 to 1700 F, either a low-carbon or a stabilized stainless steel is required. If the final anneal were above 2200 F, NbC, which is present in the niobium-stabilized Type 318 stainless steel, would be partially dissolved, and if fast cooled and later heated in the range 1000 to 1700 F the plate would contain chromium carbide. Even in Type 318 stainless steel annealed at 2150 F and fast cooled, there is some evidence that chromium-rich carbides will form in the temperature range 1200 to 1500 F. Figure 19a shows that a grain-boundary precipitate consisting of niobium carbonitrides and another phase tentatively identified as a chromium-rich carbide were present in wrought

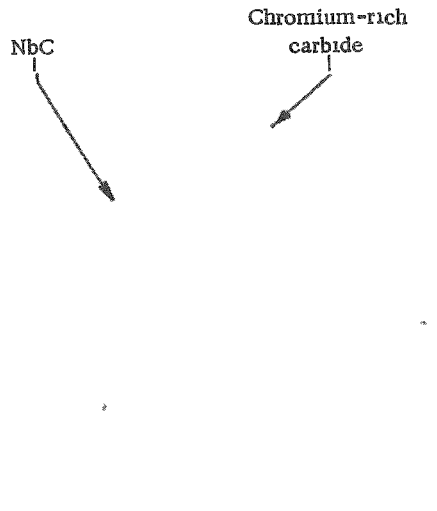

1000X Aqua Regia Etch N53488

a. Annealed 2150 F, Air Cooled, Heated 282 Hr at 1500 F

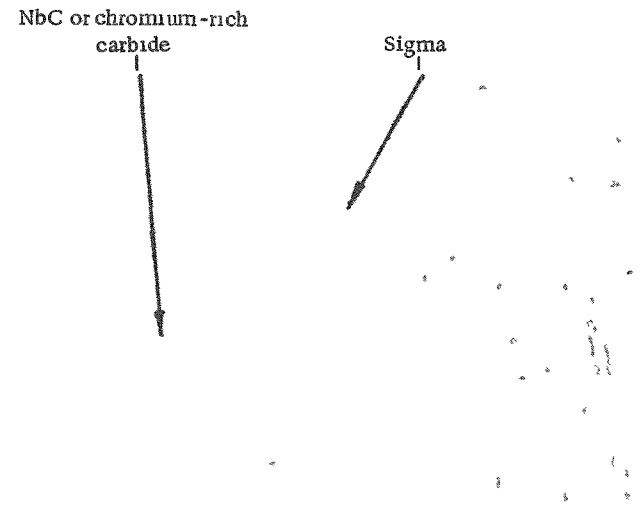

1000X Aqua Regia Etch N53494

b. Annealed 2050 F, Air Cooled, Held 2000 Hr 1500 F

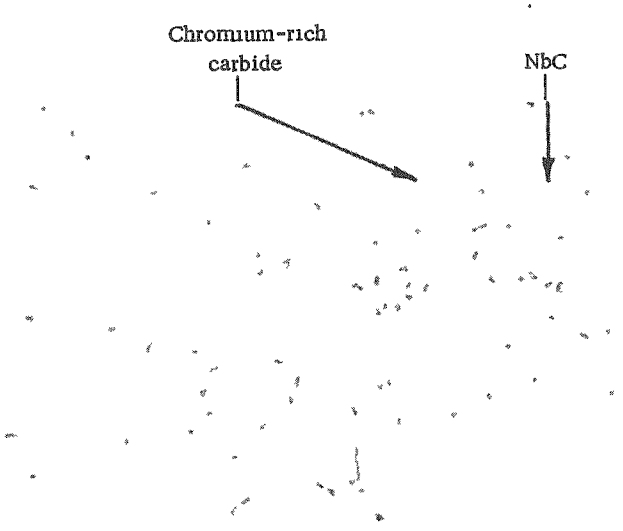

1000X Aqua Regia Etch N48740

c. Annealed 2150 F, Air Cooled, Heated 1000 Hr at 1425 F

1000X Aqua Regia Etch N50705

d. Annealed 2450 F, Held 2 Hr at 1850 F, Heated 930 Hr at 1500 F

FIGURE 19. EFFECT OF FINAL ANNEAL ON FORMATION OF CHROMIUM CARBIDES IN TYPE 318 STAINLESS AT SERVICE TEMPERATURES

Note the presence of chromium-rich carbides in grain boundaries of specimens annealed at 2150 F.

Type 318 stainless steel air cooled from 2150 F and held 282 hr at 1500 F in helium. Also shown (Figure 19b) is a specimen annealed at 2050 F, air cooled, and held 2000 hr at 1500 F which did not contain a carbide phase other than NbC. A better indication that NbC partially dissolves at 2150 F and thus does not tie up all available carbon is illustrated by the other two photomicrographs in Figure 19. A specimen (Figure 19c) annealed at 2150 F, air cooled, and held 1000 hr at 1425 F contained a grain-boundary precipitate which probably consisted of chromium-rich carbides, but a specimen (Figure 19d) annealed at 2450 F, held at 1850 F 2 hr to form NbC, and then heated 930 hr at 1500 F did not contain any carbide other than NbC. Since the experiments were originally designed for creep and corrosion tests, a closer correlation is not possible; however, Simpkinson[6] has discussed the behavior of carbides in niobium-stabilized stainless steels.

As discussed in the section on sintering, ferrite forms in the high-silicon prealloyed stainless compacts at sintering temperatures as low as 2100 F and consequently roll cladding at 2200 F and heat treating at 2050 produced no apparent decrease of ferrite. As shown in Figure 20 a short anneal at 2000 F after hot rolling or at 1900 F after cold rolling had little effect on the ferrite. Figure 20 also shows that the stringers produced by cold rolling tend to be spherodized by annealing at 2150 F. At a temperature of 1800 F or lower ferrite is rapidly converted to sigma plus austenite as shown in Figure 21.

Ferrite in elemental 18-14-2.5 matrices is not an equilibrium phase. It usually exists near the edge of undissolved chromium particles and can be placed in solution by proper heat treatment. The standard procedure of hot rolling at 2200 F, annealing at 2000 to 2200 F, cold rolling, and annealing at 2050 F is not sufficient to dissolve the chromium-rich areas. As shown in Figure 22, even long-time anneals at 2200 F did not place all the chromium in solution. However, as shown in Figure 23, a 2-hr anneal at 2300 F resulted in a single-phase structure regardless of whether the plate was annealed before or after cold rolling. When the chromium powders are not screened, large agglomerates may be included in the structure which do not go into solution even when the plate is annealed at 2300 F (Figure 24). The anneal is more reliable after cold rolling, since diffusion of the chromium is more rapid, but if the 2300 F anneal is the final heat treatment extremely large grains (some the full width of the cladding) occur in the cladding.

Sigma did not occur in as-fabricated fuel elements since fabrication and required heat-treatment temperatures were well above the temperature at which sigma is stable. However, sigma can form (particularly in molybdenum-bearing stainless steels) if annealing or service temperatures of 1200 to 1700 F are used. The presence of impurities or secondary phases may also promote the formation of sigma. For example, as shown in Figure 21, ferrite in high-silicon prealloyed Type 318 stainless steel transformed to sigma plus austenite after a short time at temperatures as high as 1800 F. A temperature of 1713 F was the highest temperature at which sigma was detected in commercial wrought Type 318 stainless which did not contain ferrite prior to heat treating (Figure 25). After 1622 hr, a 10 volume per cent precipitate of sigma was present — mostly in the grain boundaries.

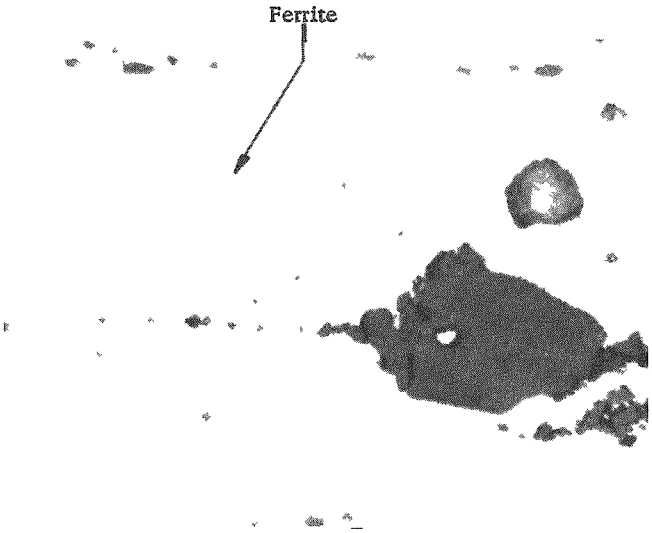

1000X Aqua Regia Etch N46322

a. Hot Rolled at 2200 F and Annealed 2 Hr at 2000 F

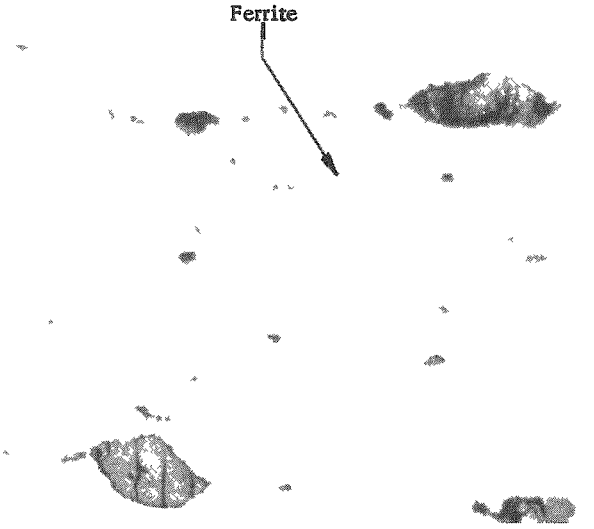

1000X Aqua Regia Etch N46320

b. Hot Rolled 2200 F, Annealed at 2000 F, and Cold Reduced 20 Per Cent in Thickness.

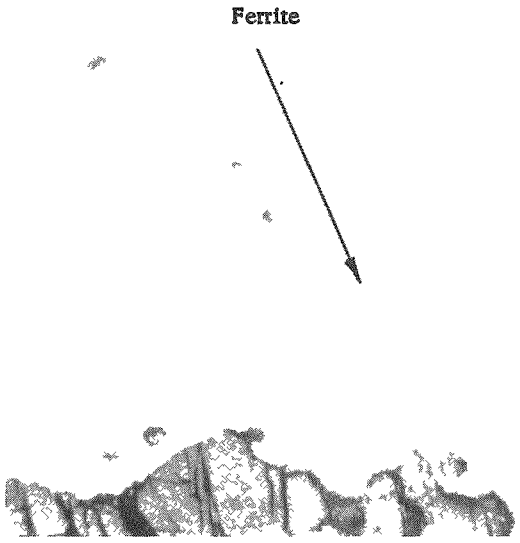

1000X Aqua Regia Etch N46321

c. Annealed 45 Min at 2150 F After Cold Rolling

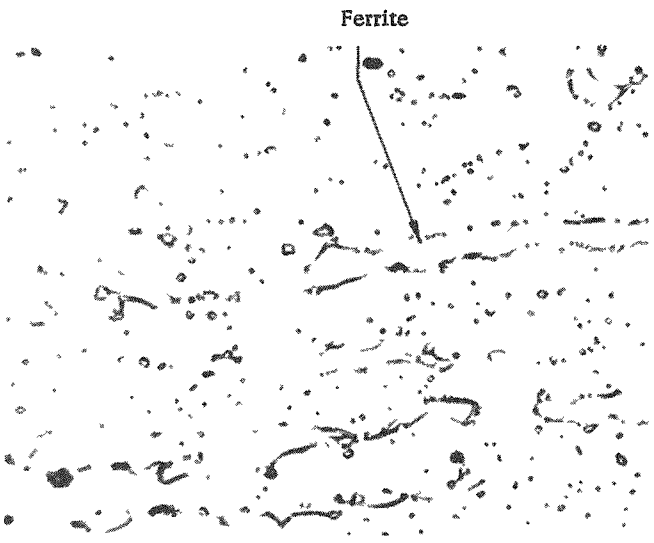

1000X Chromic Electrolytic Etch N44912

d. Annealed 45 Min at 1900 F After Cold Rolling

FIGURE 20. FERRITE IN FUEL ELEMENTS MADE WITH HIGH-SILICON PREALLOYED TYPE 318 STAINLESS STEEL POWDER

Annealing at 2000 or 1900 F has little effect on ferrite. Stringers produced by cold rolling tend to be spherodized by annealing at 2150 F.

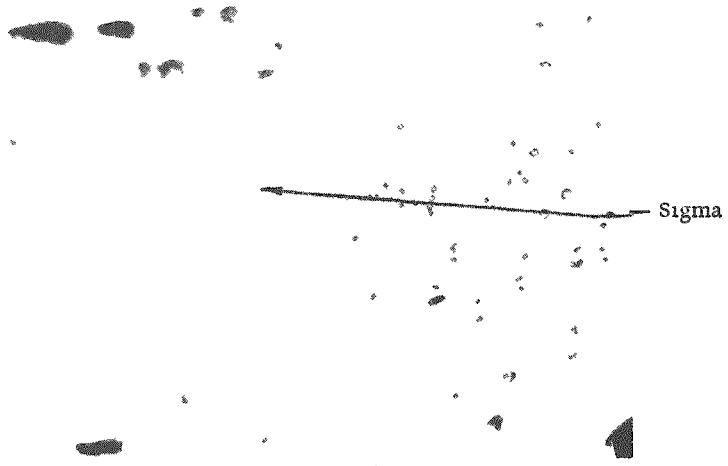

1000X Sodium Cyanide Electrolytic Etch N44916

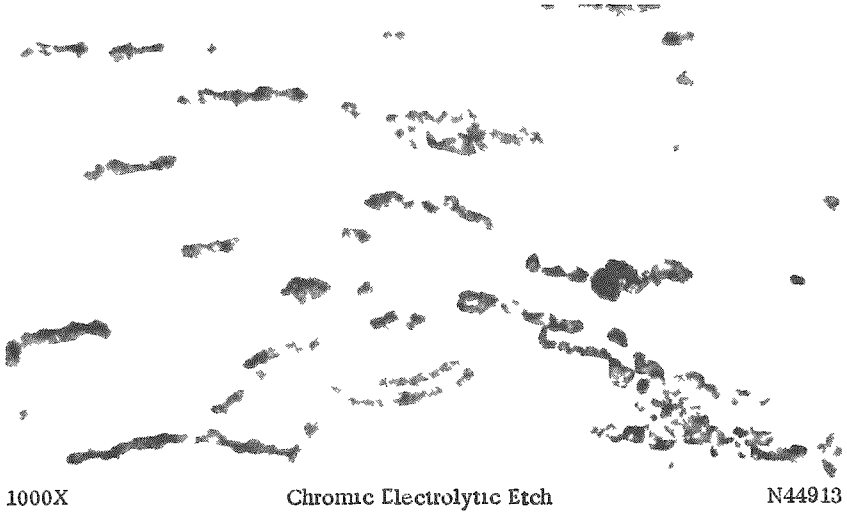

1000X Chromic Electrolytic Etch N44913
(Sigma Selectively Attacked)

FIGURE 21. SIGMA, PRODUCED BY THE TRANSFORMATION OF FERRITE TO SIGMA PLUS AUSTENITE BY ANNEALING 45 MIN AT 1800 F AFTER COLD ROLLING, IN FUEL ELEMENTS CONTAINING A HIGH-SILICON PREALLOYED TYPE 318 STAINLESS POWDER MATRIX

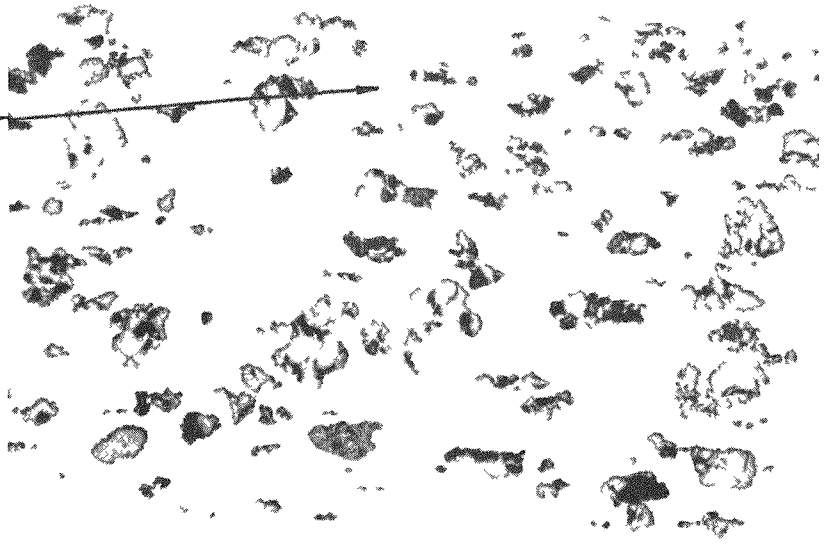

100X Aqua Regia Etch N46786

a. Annealed 2 Hr at 2200 F

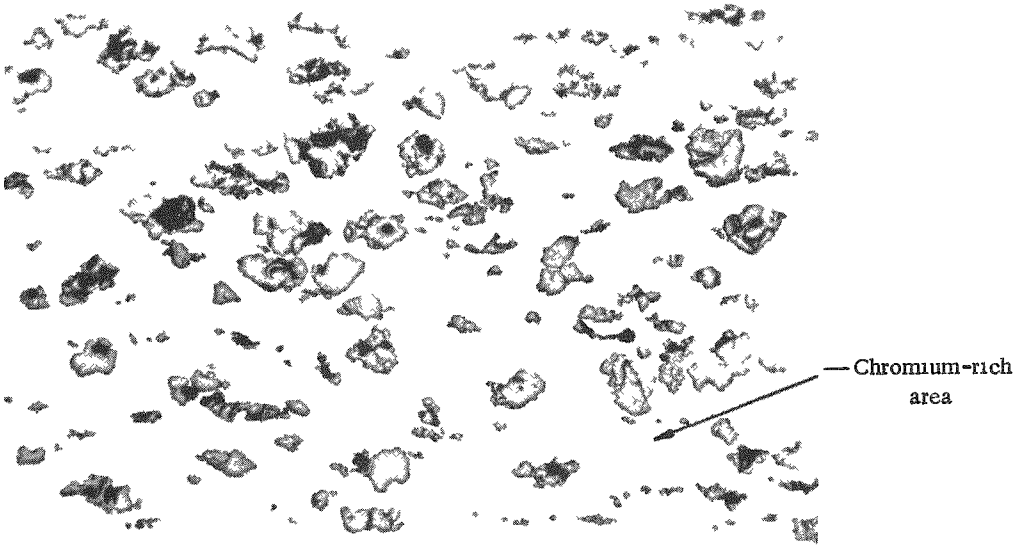

100X Aqua Regia Etch N46785

b. Annealed 40 Hr at 2200 F

FIGURE 22. EFFECT OF ANNEALING AT 2200 F ON CHROMIUM SOLUTION IN 18-14-2.5 ALLOY MATRICES

As can be seen, even 40-hr annealing at 2200 F did not place all chromium in solution. Specimens were sintered at 2200 F, hot roll clad at 2200 F, annealed at 2200 F, and cold rolled to a 20 per cent reduction in thickness. (Transverse sections)

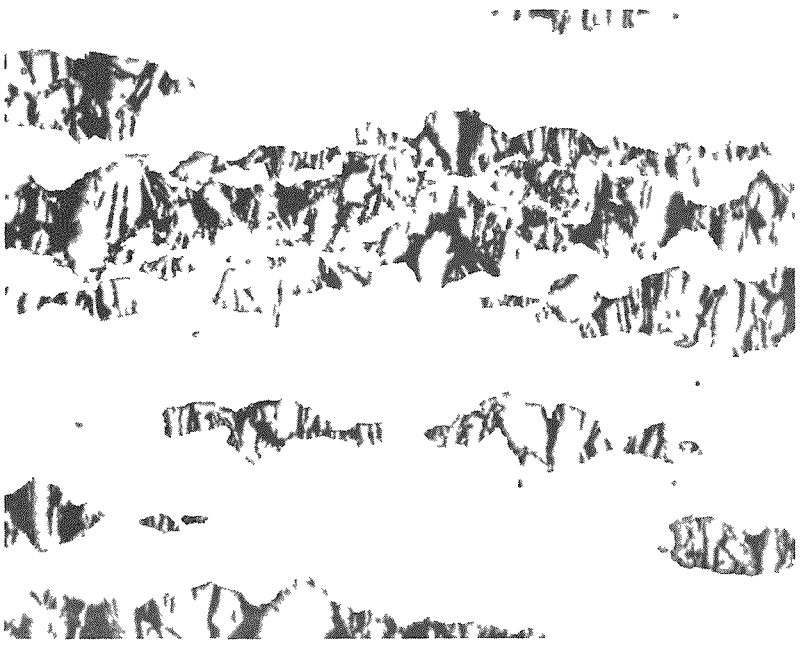

250X Aqua Regia Etch RM10174

a. Annealed 2 Hr at 2300 F, Cold Rolled to 21 Per Cent Reduction in Thickness, Annealed 1 Hr at 2050 F

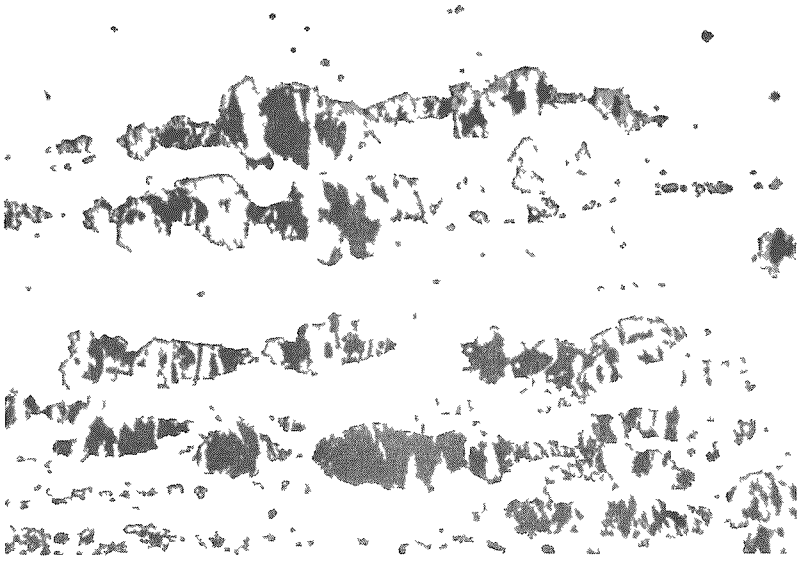

250X Aqua Regia Etch RM9421

b. Annealed 2 Hr at 2000 F, Cold Rolled to 21 Per Cent Reduction in Thickness, Annealed 2 Hr at 2300 F

FIGURE 23. EFFECT OF ANNEALING AT 2300 F ON CHROMIUM SOLUTION IN 18-14-2.5 ALLOY

Annealing at 2300 F resulted in a single-phase structure regardless of whether the plate was annealed before or after cold rolling. Specimens were sintered at 2300 F and hot roll clad at 2200 F.

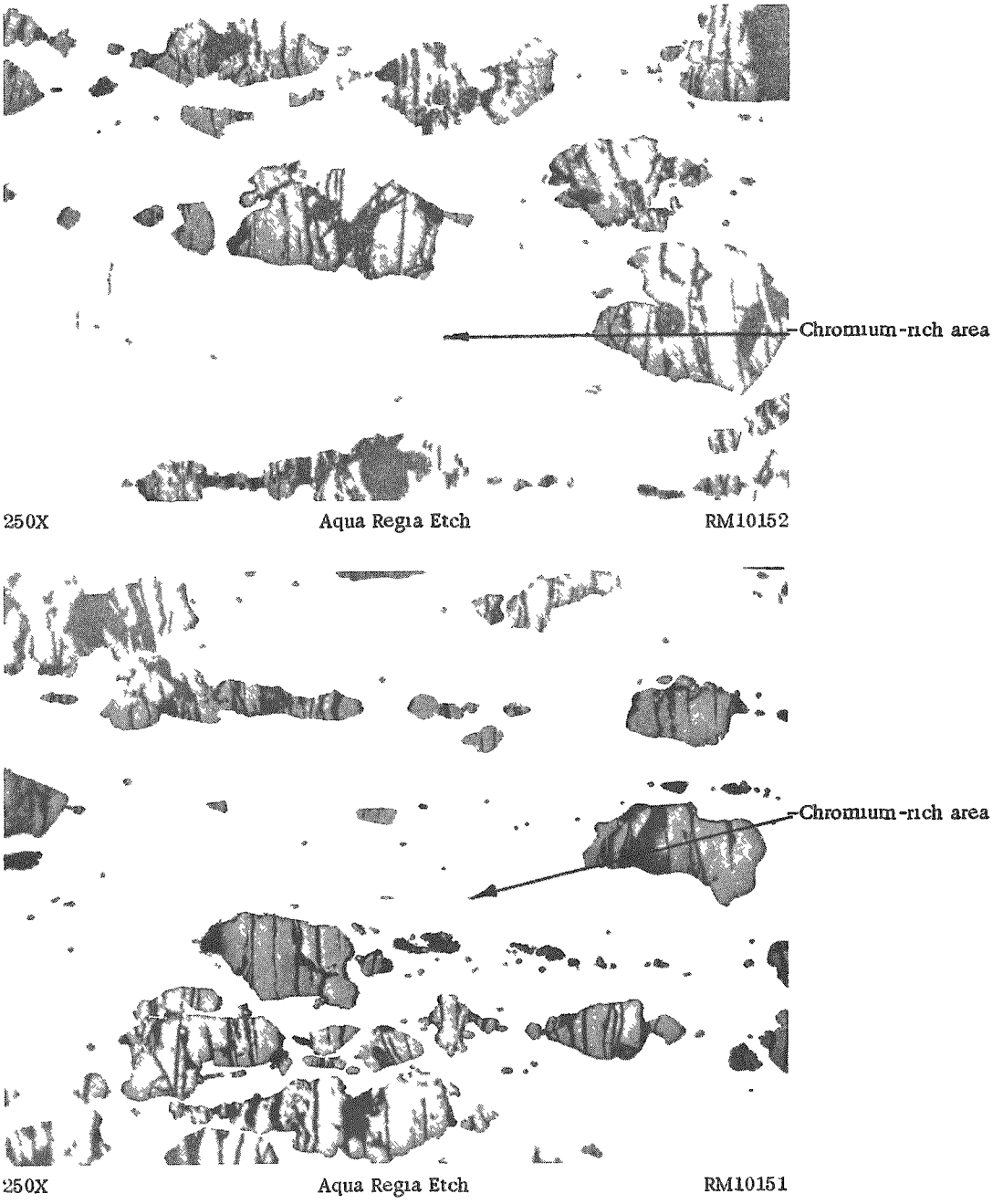

FIGURE 24. CHROMIUM-RICH AREAS IN FABRICATED FUEL ELEMENTS WITH AN 18-14-2.5 ALLOY MATRIX

Annealing for 2 hr was not sufficient to dissolve the large chromium particles. Plates were annealed 2 hr at 2300 F prior to cold rolling. Unscreened chromium powder containing large agglomerates of chromium was used to mix the matrix.

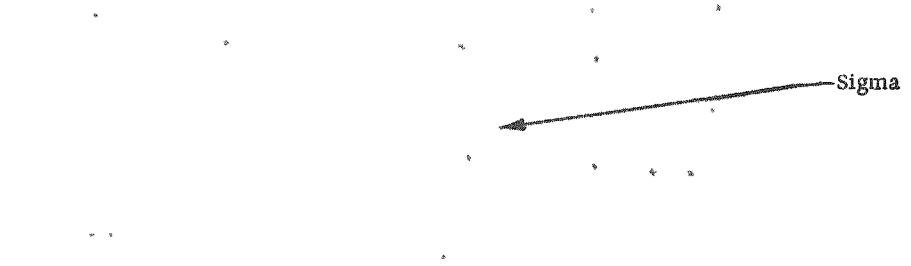

500X Aqua Regia Etch N48737

a. Wrought Type 318 Stainless, Annealed 2150 F, and Heated 1622 Hr in NaK at 1713 F

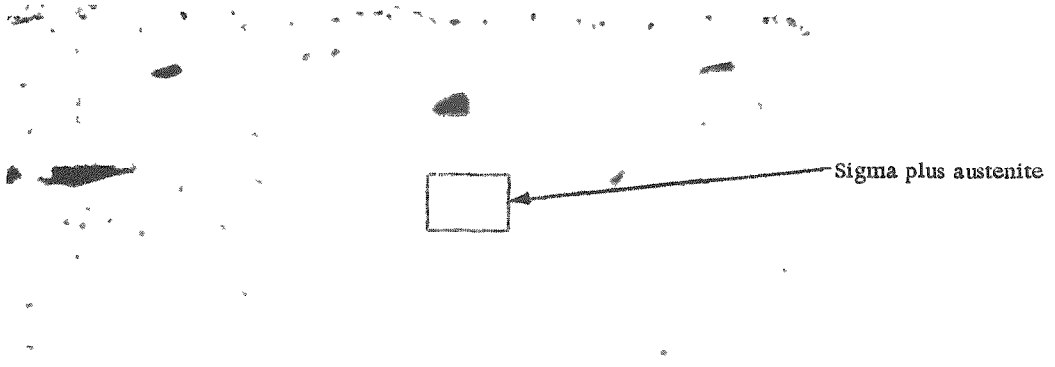

1000X Sodium Cyanide Electrolytic Etch N44915

b. Prealloyed High-Silicon Type 318 Stainless Hot Rolled 2200 F, Cold Reduced 15 Per Cent in Thickness, and Heated 2 Hr at 1500 F

1000X Aqua Regia Etch N53495

c. Elemental 18-14-2.5 Alloy, Annealed 2050 F, and Held 2000 Hr at 1500 F

FIGURE 25. EXAMPLES OF SIGMA PHASE IN FUEL ELEMENTS

At 1500 F sigma was present in the wrought alloy after 282 hr, but approximately 10 volume per cent sigma could be detected in a specimen heated for 2000 hr (see Figure 19). Two hours at 1500 F after 15 per cent cold work was sufficient to transform ferrite in high-silicon prealloyed Type 318 powder compacts to sigma plus austenite (Figure 25). The cold work is not considered necessary since annealing at 2150 F and furnace cooling was observed to transform the ferrite. Sigma can also form in the 18-14-2.5 elemental matrix but since the impurity level is low, the alloy is less susceptible — particularly since the sigma must form from austenite or chromium-rich areas. After 2000 hr at 1500 F, a specimen containing some chromium segregation contained about 5 volume per cent of sigma (Figure 25). Another phase, present in small amounts in some of these structures, could not be positively identified but may be the chi phase reported by some investigators.[7] Sigma formation can be partially suppressed by removing the molybdenum, but a lower strength fuel element will result. Sigma-phase formation has been the subject of many investigations[7,8,9], but its effect on mechanical properties or resistance to irradiation at elevated temperatures has not been determined. Creep-strength data presented in the next section indicate that no detrimental effects occurred due to the presence of sigma, and the creep strength may actually have been increased.

Oxide formation has been discussed in the section on sintering. Oxides are not formed or reduced during roll cladding and heat treating, but are usually broken up and stringered.

A final anneal after cold rolling is not only useful for flat annealing, recrystallizing the grains, and converting the carbon to niobium carbide, but it is also necessary if bend ductility is desired. Plates subjected to bend tests after cold rolling showed little or no bend ductility. As indicated in Table 11, short anneals at any temperature above 1900 F resulted in the maximum bend ductility for prealloyed matrix plates. Cooling rates did not appear to affect the bend ductility.

RELATIONSHIP OF OTHER VARIABLES

In general, changes in roll-cladding procedures tended to produce the same effects regardless of how the UO_2-stainless steel core compacts were produced. Thus, optimum hot-rolling and cold-rolling techniques for a particular UO_2-stainless steel dispersion are very likely to be optimum for similar UO_2-stainless steel dispersions prepared from different materials or by different procedures. However, the actual appearance of the microstructure, the mechanical properties, and probably the resistance to corrosion and irradiation depend to a great extent on the materials used and the method of core preparation. The effects of variation in particle size and type of both UO_2 and metal powders and in densities of core compacts prior to rolling were considered. Variations in core preparation as related to obtaining cores with a uniform distribution of UO_2 and a particular core density were discussed in a previous section.

TABLE 11. EFFECT OF ANNEALING CONDITIONS ON THE BEND DUCTILITY OF 25 w/o UO_2-STAINLESS FUEL ELEMENTS

Core-Matrix Material	UO_2 Particle Size, μ	Annealing Conditions	Bend Rating, T
		Effect of Annealing Temperature After Cold Rolling	
Prealloyed Type 318 stainless	50-75	15 min at 2250 F	4.2
	50-75	45 min at 2150 F	4.2
	50-75	45 min at 2150 F plus 2 hr at 1500 F	4.2
	50-75	45 min at 2025 F	4.2
	50-75	45 min at 1900 F	4.2
	50-75	45 min at 1800 F	5.6
	50-75	45 min at 1700 F	5.6
	50-75	2 hr at 1500 F	> 8.3
	50-75	As cold rolled	> 8.3
		Effect of Cooling Rate From Annealing Temperature	
Prealloyed Type 318 stainless	50-75	10 min at 2150 F, slow cool	4.2
	50-75	10 min at 2150 F, fast cool	4.2
Elemental 18-14-2.5 alloy	75-105	10 min at 2150 F, slow cool	1.4
	75-105	10 min at 2150 F, fast cool	1.4

Core Densities

When cores of low densities were roll clad the stringering of UO_2 particles was pronounced. Apparently the UO_2 was free to move, at least on the first pass, and tended to line up in the rolling direction. In the high-density compacts, as the metal surrounding a particular UO_2 particle flowed it carried the UO_2 particle along to a certain extent and the stringering was reduced. As shown in Figure 26, stringering was severe for compacts of less than 80 per cent of theoretical density prior to roll cladding. Results in this investigation indicated that good dispersions could be obtained if the densities were 85 per cent of theoretical or higher prior to roll cladding. The main difference in fabrication of compacts to get the different densities and structures of the specimens in Figures 26a and 26b was the coining of the specimen in Figure 26b after sintering. Compacts with elemental matrices are not as severely affected by density variations, but, as shown in Figure 27, green compacts result in severe stringering regardless of the matrix used.

Matrix Particle Size

As discussed in the section on sintering, if elemental powders are used, it is desirable to use fine powders in order to promote diffusion; therefore, elemental powders of minus 325-mesh size were used consistently. No marked improvement was noted when minus 400-mesh powder was used (Figure 28).

As received minus 100-mesh powder was used throughout the investigation for most of the work with prealloyed powders. However, as shown in Figure 29, better dispersions could be obtained with the finer powders.

Comparison of Elemental and Prealloyed Matrices

Although a variation in a particular operation will usually affect the structure in a similar manner regardless of whether the matrix is prepared from elemental or prealloyed powders, slight variations in procedure cause a more severe change in the structure of elements containing prealloyed powders. The difference in structure is partially due to the difference in ductility. In Figure 30 comparative structures of prealloyed- and elemental-matrix elements are shown. The plates were fabricated under the most favorable conditions for prealloyed elements; i. e., use of a high sintering temperature (2300 F), which reduces carbon, increases ferrite, and improves ductility, and use of fine metal powders. Even under these conditions stringering and fracturing of UO_2 is more severe when prealloyed Type 318 powder is used. The Type 302B powder is more ductile and a better structure results, but the elemental matrix, even though it contains 2.5 w/o molybdenum, has a slightly better dispersion. If a 2200 F sintering temperature is used to reduce the amount of ferrite formed, the difference in structures is more noticeable, as shown in Figure 31.

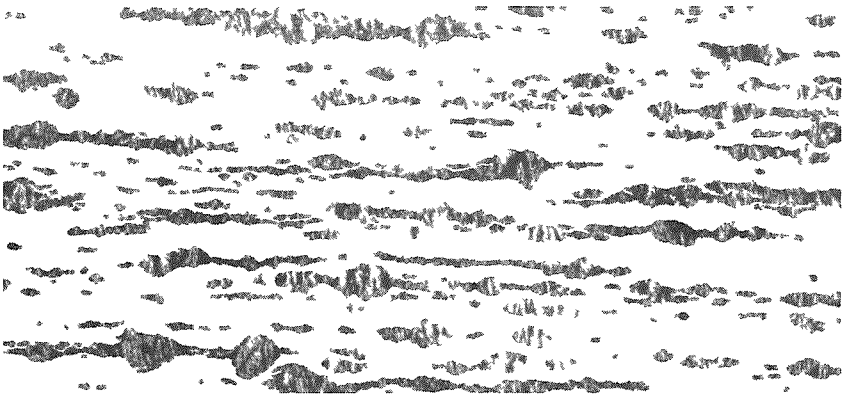

100X As Polished RM8761

a. 78 Per Cent of Theoretical Density

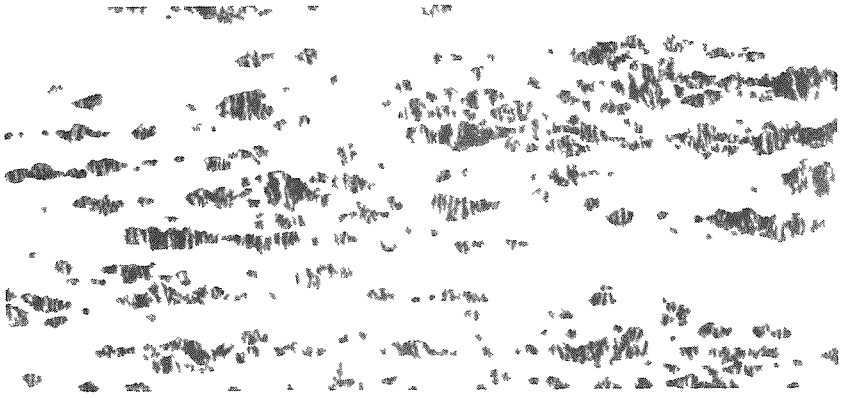

100X As Polished RM8767

b. 82 Per Cent of Theoretical Density

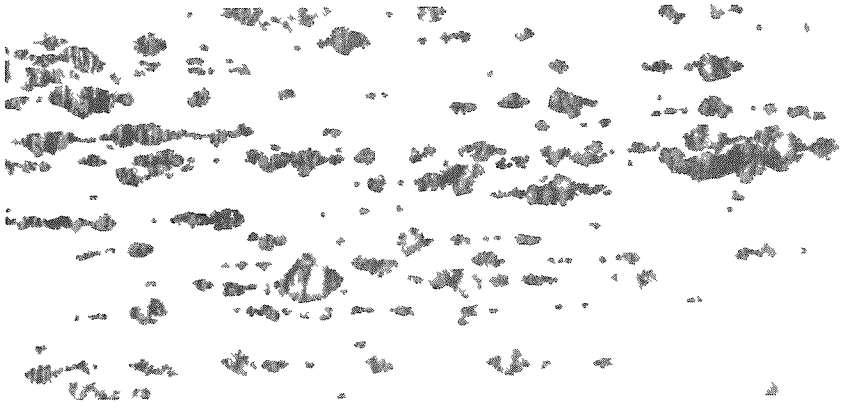

100X As Polished RM8809

c. 90 Per Cent of Theoretical Density

FIGURE 26. EFFECT OF COMPACT DENSITY ON ROLL-CLAD STRUCTURE OF 25 w/o UO_2 (MINUS 200 PLUS 270-MESH) DISPERSED IN A TYPE 318 PREALLOYED STAINLESS STEEL POWDER MATRIX

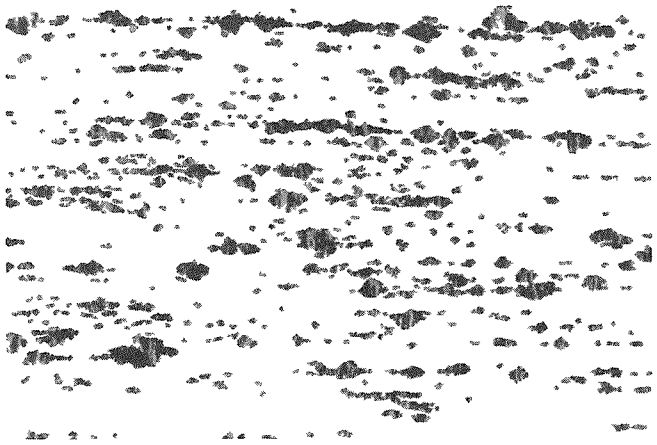

100X As Polished RM8679

100X As Polished RM5962

a. Specimens Roll Clad After Cold Pressing

20 w/o UO_2 (minus 200 plus 270-mesh size) in a Type 318 prealloyed matrix. Roll clad green after pressing at 50 tsi to 76 per cent of theoretical density.

25 w/o UO_2 (minus 100 plus 200-mesh size) in an 18-14-2.5 alloy elemental matrix. Roll clad green after cold pressing at 40 tsi to 78.5 per cent of theoretical density.

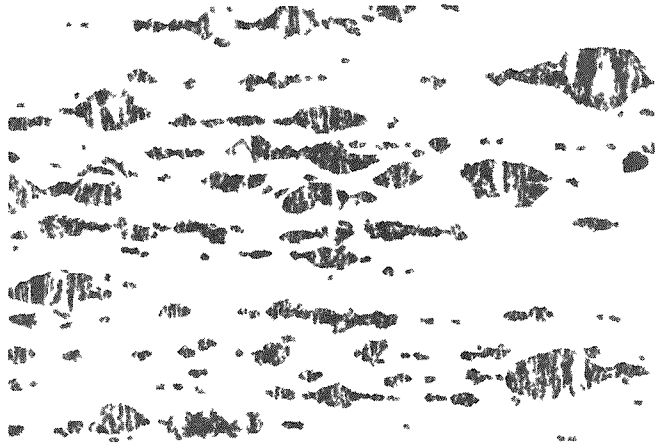

100X As Polished RM8579

100X As Polished RM5961

b. Specimens Roll Clad After Sintering

20 w/o UO_2 (minus 200 plus 270-mesh size) in a Type 318 prealloyed matrix. Core pressed at 50 tsi, sintered for 4 hr at 2200 F, and coined at 50 tsi to 86.8 per cent of theoretical density.

25 w/o UO_2 (minus 100 plus 200-mesh size) in an 18-14-2.5 alloy elemental matrix. Roll clad after sintering at 2200 F to 89.5 per cent of theoretical density.

FIGURE 27. COMPARISON OF ROLL-CLAD CORES MADE FROM GREEN AND SINTERED COMPACTS

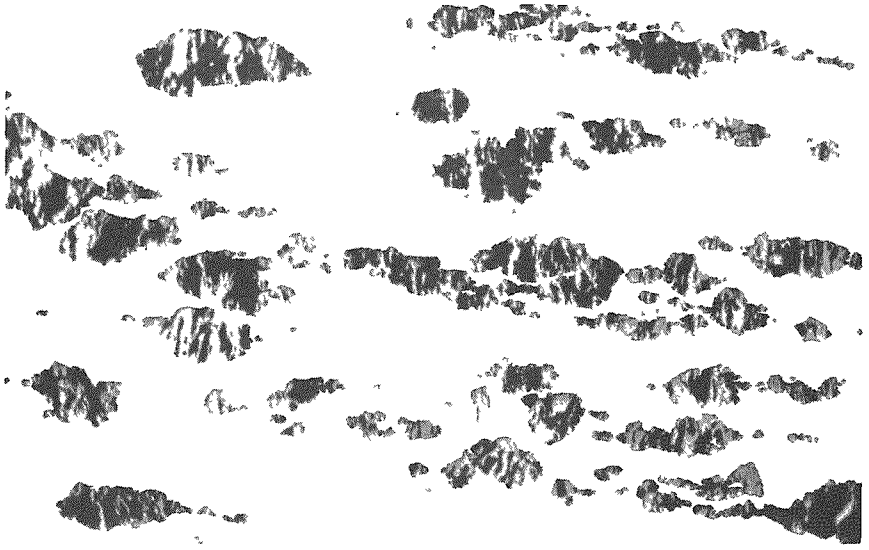

100X As Polished RM9914

a. Minus 325 Plus 400-Mesh Matrix Particles

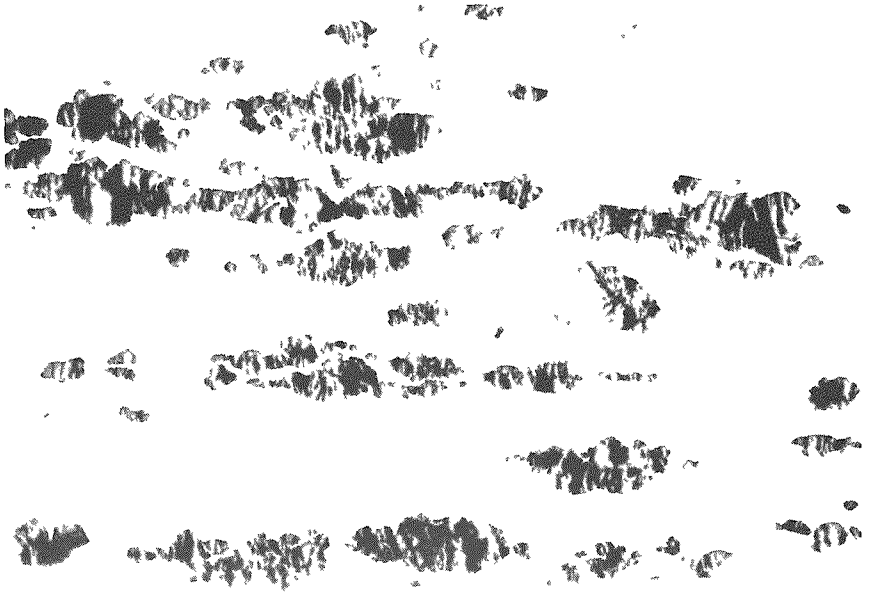

100X As Polished RM9915

b. Minus 400-Mesh Matrix Particles

FIGURE 28. EFFECT OF MATRIX POWDER SIZE ON THE STRUCTURE OF FUEL ELEMENTS CONTAINING 25 w/o UO_2 (MINUS 100 PLUS 400 MESH) IN AN ELEMENTAL 18-14-2.5 ALLOY MATRIX

In cores made from elemental powder mixtures, fine particle sizes are desirable to promote diffusion. However, as is evident in the photomicrographs, no marked improvement in structure was produced by use of a minus 400-mesh instead of the standard minus 325-mesh particle size. Compacts were sintered at 2300 F, roll clad at 2200 F, and cold reduced 20 per cent in thickness.

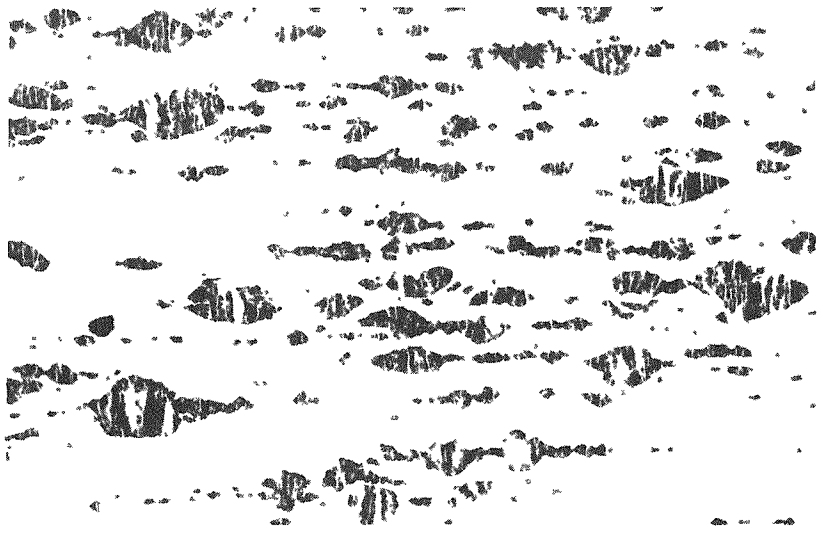

100X As Polished RM8579

a. Matrix has minus 100-mesh size powder (approximately 30 w/o is minus 325-mesh size).

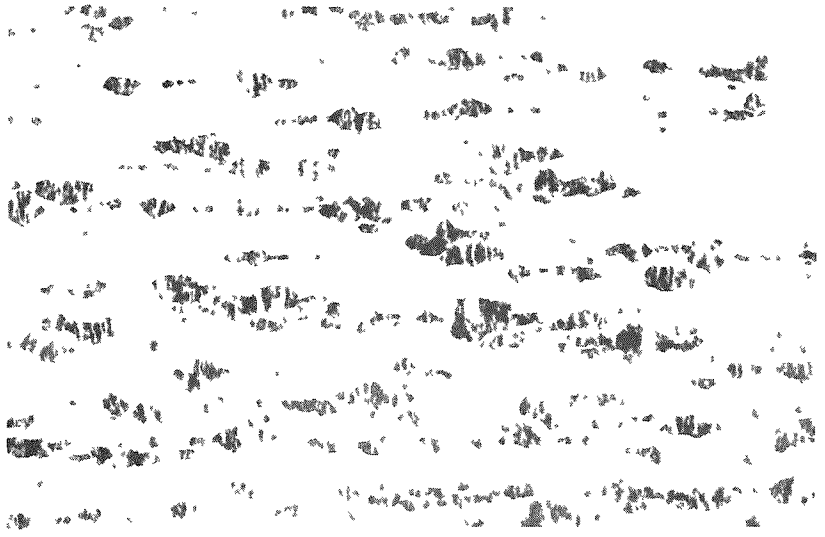

100X As Polished RM8677

b. Matrix has 80 w/o minus 325-mesh size, 20 w/o minus 100 plus 140 mesh size.

FIGURE 29. EFFECT OF MATRIX PARTICLE SIZE ON STRUCTURE OF FUEL ELEMENTS CONTAINING 20 w/o UO_2 IN TYPE 318 STAINLESS PREALLOYED POWDER

For prealloyed powder matrices, minus 100-mesh particles give satisfactory results, but, as can be seen, a finer particle size can give a better dispersion. Compacts were sintered at 2200 F, roll clad at 2200 F, and cold reduced 20 per cent in thickness.

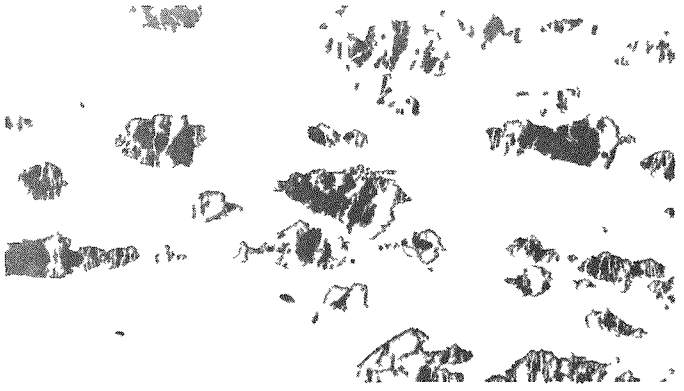

100X As Polished RM11076

a. Elemental 18-14-2.5 Matrix

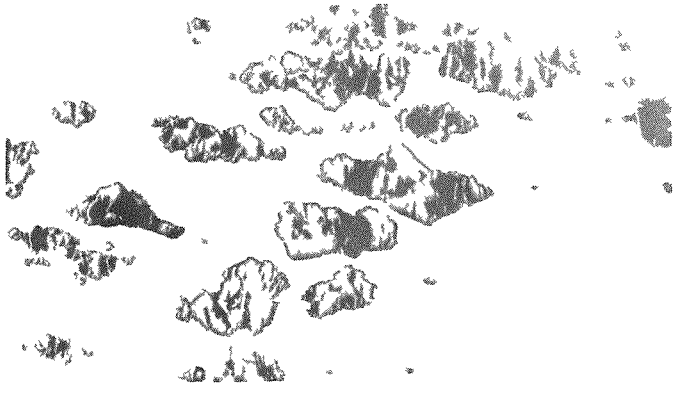

100X As Polished RM11080

b. Prealloyed Type 302B Matrix

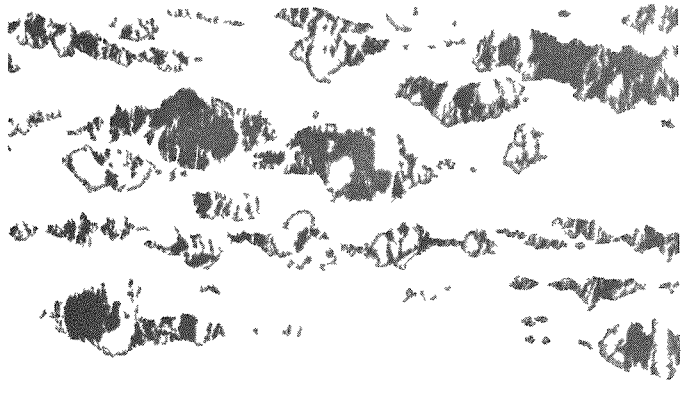

100X As Polished RM11078

c. Prealloyed Type 318 Matrix

FIGURE 30. THE EFFECT OF VARIATION IN MATRIX MATERIAL ON FUEL-ELEMENT STRUCTURES

Specimens contain 25 w/o minus 100 plus 140-mesh UO_2. Matrix powder of minus 325 plus 400 mesh was used. Compacts were sintered at 2300 F, roll clad at 2200 F, and cold reduced 20 per cent in thickness.

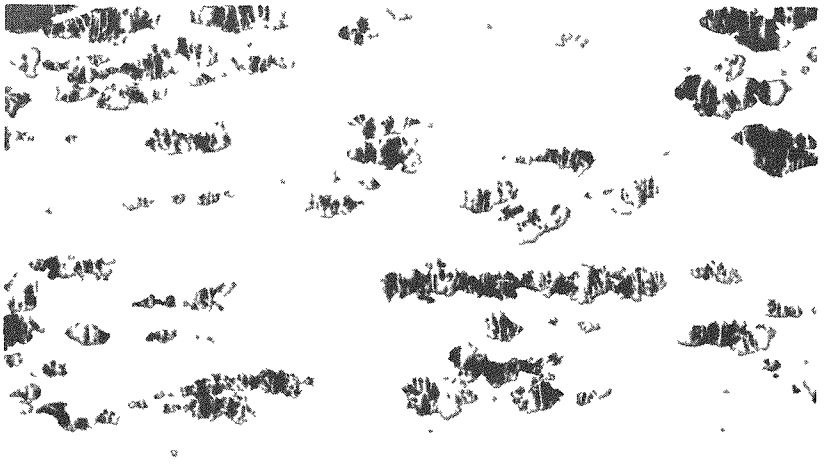

100X As Polished RM9924

a. 18-14-2.5 Alloy Matrix Compact Sintered at 2300 F

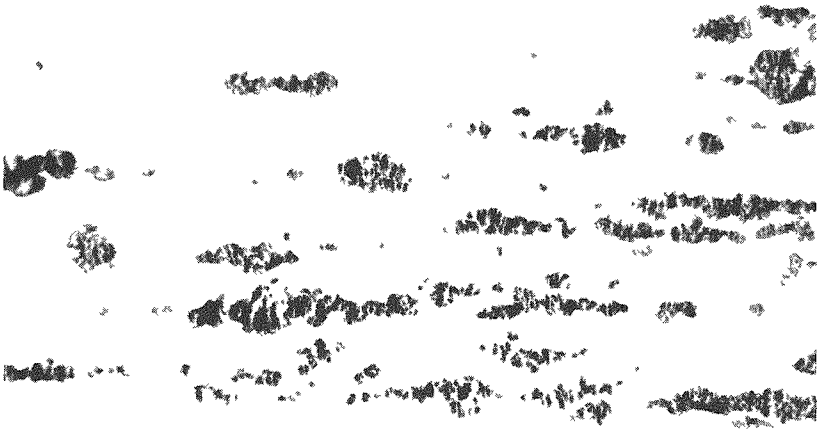

100X As Polished N53879

b. Type 318 Prealloyed Stainless Matrix Compact Sintered at 2200 F

FIGURE 31. COMPARISON OF ELEMENTAL AND PREALLOYED MATRICES

The superiority of the elemental matrix evident in Figure 30a becomes more noticeable when a sintering temperature of 2200 F is employed to reduce the amount of ferrite formed in the prealloyed powder. 25 w/o UO_2 (minus 100 plus 140 mesh) dispersed in minus 325-mesh matrix powders. Roll clad at 2200 F and cold rolled to a 20 per cent reduction in thickness.

By the use of minus 325-mesh prealloyed powder, minus 100 plus 140-mesh UO_2, and fabrication under optimum conditions, fuel elements having room-temperature bend ductility equal to that for elemental-matrix powders (1.4T) can be achieved. However, the prealloyed powders are more sensitive to fabrication variables and prealloyed-matrix elements fabricated in this investigation varied in bend ductility from ratings of 1.4T to 5.6T, with the average being 4.2T. Elemental matrix plates had an average T-rating of 1.4, with the worst ductility obtained in this investigation being 2.8T.

Because of stringering and fracturing of UO_2, it would be expected that the cores would have directional properties with the lowest strength being in the thickness direction. Comparisons of tensile strengths measured in the thickness direction are shown in Table 12. It is clear that dispersions of UO_2 in elemental matrices have higher strengths. This higher strength must be attributed to less stringering and fracturing of UO_2 since, as indicated in Table 13, when specimens are pulled in tension in the direction of rolling, the tensile strength of the prealloyed-matrix plates is slightly better at room temperature. The higher strength of both types of plates is partially due to the strength of the cladding, which occupies 30 per cent of the cross-sectional area. At temperatures below 1650 F, the tensile strength of prealloyed specimens is slightly higher than for elemental specimens. However, at the time the tests were run the only elemental plates available contained Cr_2O_3. It would be expected that tensile strength would increase with a decrease in oxide as indicated both by the poor strengths of chromite-containing low-silicon prealloyed specimens and the higher tensile strengths of specimens which do not contain UO_2.

TABLE 12. COMPARISON OF TRANSVERSE TENSILE STRENGTH OF FUEL ELEMENTS CONTAINING PREALLOYED MATRICES AND ELEMENTAL MATRICES

Composition	Temperature, F	UO_2 Particle Size, μ	Transverse Tensile Strength, psi
25 w/o UO_2 in Type 318 prealloyed stainless	Room	75-105	15,400
	1000	75-105	11,900
	1300	75-105	10,200
25 w/o UO_2 in elemental 18-14-2.5 alloy	Room	75-150	24,700
	1000	75-150	16,900
	1300	75-150	14,400

TABLE 13. COMPARISON OF HOT TENSILE STRENGTH OF VARIOUS FUEL PLATES WITH PLATES CONTAINING NO UO_2[a]

Material	Temperature, F	Ultimate Tensile Strength[b], psi	Elongation in 2 In.[b], per cent
Commercial Type 318 stainless steel sheet	Room	81,000	61
	1350	45,000	37
	1500	30,000	27
	1650	17,500	35
Prealloyed Type 318 stainless core, no UO_2	Room	96,000	53
	1350	41,000	45
	1500	28,000	30
	1650	15,000	42
Elemental 18-14-2.5 alloy core, no UO_2	Room	79,000	40
	1350	35,000	28
	1500	22,000	20
	1650	13,000	13
25 w/o UO_2-elemental 18-14-2.5 alloy core	Room	60,700	9
	1350	28,200	12
	1500	20,200	10
	1650	14,200	8
25 w/o UO_2-prealloyed high-silicon Type 318 stainless core	Room	62,000	10
	1350	36,500	10
	1500	23,000	13
	1650	13,000	13
25 w/o UO_2-prealloyed low-silicon Type 318 stainless core	Room	45,000	4
	1350	30,000	3
	1500	23,000	4
	1650	14,500	6

(a) Fueled cores are 0.031 in. thick and plates have 0.005-in. cladding. Core edges are exposed.
(b) Average of three or more tests.

The creep strength as indicated by the stress-to-rupture curves in Figure 32 is higher at 1500 and 1650 F for fuel elements containing prealloyed matrices. All elemental plates used contained Cr_2O_3 which may have decreased the strength. It is interesting to note that prealloyed plates contained from 5 to 10 volume per cent sigma which did not appear to be detrimental and may actually have increased creep resistance. The curves also show that the addition of molybdenum to the core and the use of Type 318 stainless cladding increased the creep resistance.

UO_2 Particle Size

It is usually considered preferable to have UO_2 particles of 50 μ or more in diameter so that radiation damage due to recoil will not be continuous in the matrix. Good dispersions can be produced with any particle size UO_2 in the range 50 to 150 μ in diameter, but, as shown in Figure 33, there appears to be less tendency for stringering with larger particles. As shown in Figure 34, particles of a wide range of sizes can be used to obtain good dispersions. It should be noted, however, that the greatest percentage of UO_2 particles are relatively large. Table 14 indicates that decreasing the particle size increases transverse tensile strength (measured in the thickness direction of the plate) but decreases room-temperature bend ductility. As confirmed by microstructures and the bend-ductility values, the increase in tensile strength is not due to an improved dispersion of UO_2, but the cross-sectional area of metal subjected to tension is probably more uniform across the thickness direction of the plate.

TABLE 14. EFFECT OF UO_2 PARTICLE SIZE ON TRANSVERSE TENSILE STRENGTH AND BEND DUCTILITY

Core Composition	UO_2 Particle Size, μ	Transverse Tensile Strength, psi	Bend Ductility, T
25 w/o UO_2 in elemental 18-14-2.5 alloy	<44	30,500	--
	44-50	--	0.5
	50-75	--	1.0
	75-105	--	1.0
	105-150	--	1.0 to 1.6
	75-150	24,700	--
25 w/o UO_2 in prealloyed Type 318 stainless	<44	18,000	--
	50-75	16,000	4.2
	75-105	15,400	2.8
	100-150	14,200	1.4[a]

(a) Plate contained minus 325-mesh prealloyed powder.

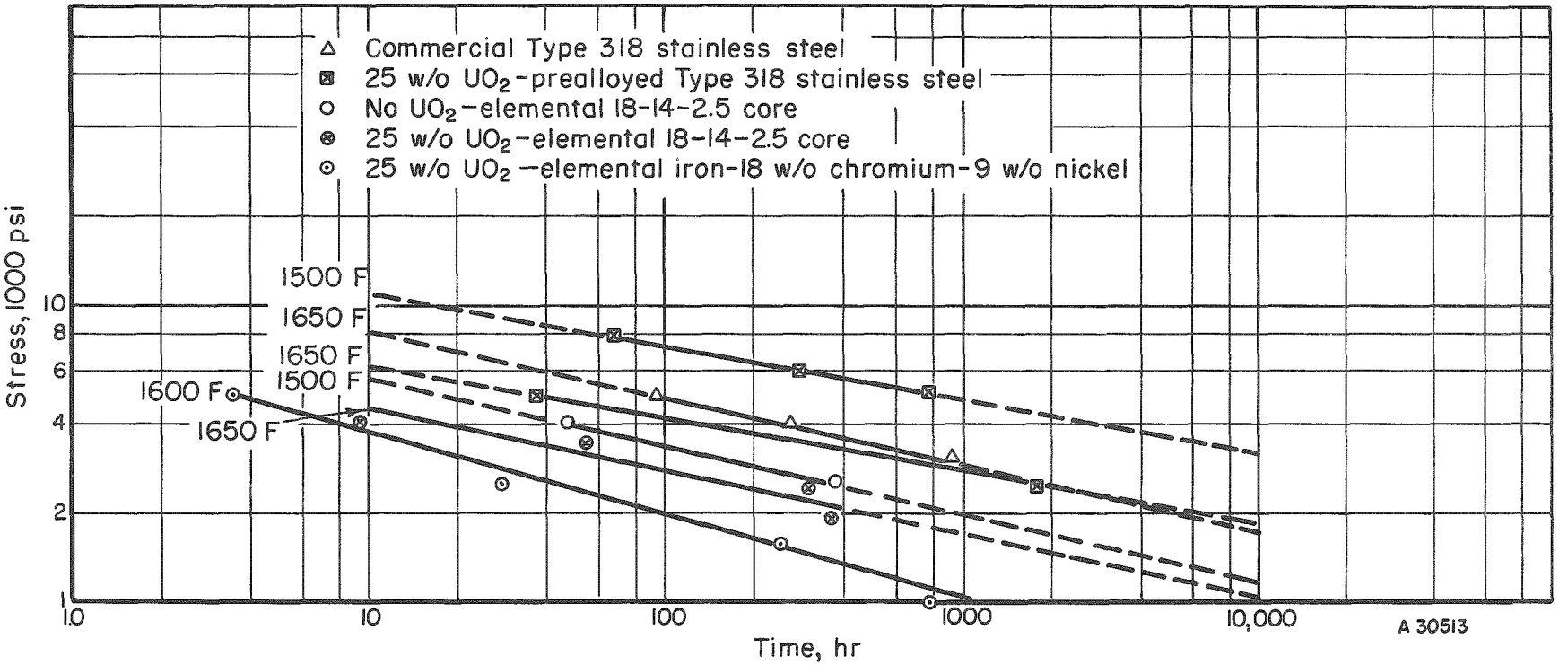

FIGURE 32. STRESS-RUPTURE CURVES FOR VARIOUS UO_2 FUEL PLATES COMPARED WITH PLATE NOT CONTAINING UO_2

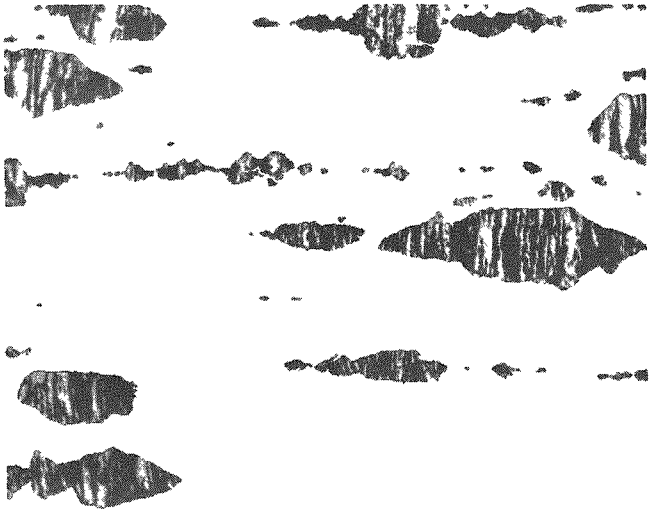

100X As Polished RM8580

a. Minus 100 Plus 150-Mesh UO_2

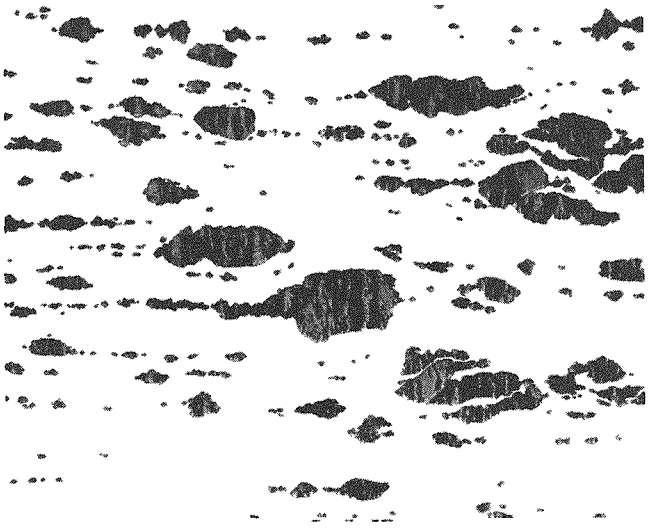

100X As Polished RM8578

b. Minus 150 Plus 200-Mesh UO_2

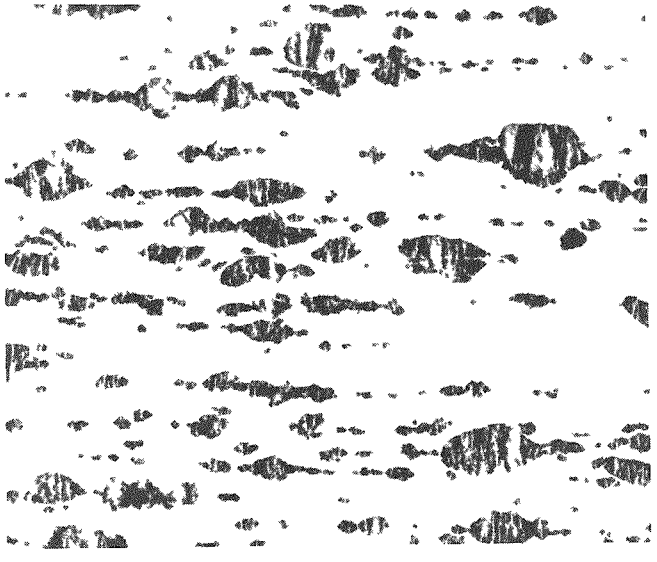

100X As Polished RM8579

c. Minus 200 Plus 270-Mesh UO_2

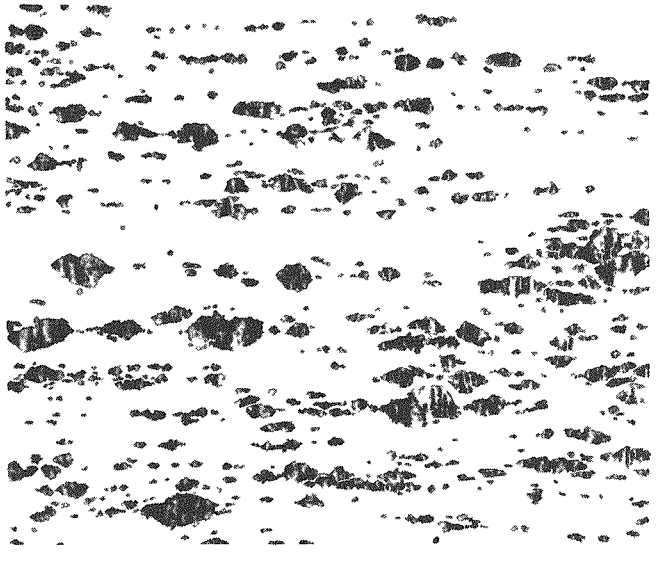

100X As Polished RM8577

d. Minus 270 Plus 325-Mesh UO_2

FIGURE 33. EFFECT OF UO_2 PARTICLE SIZE ON STRUCTURE OF FUEL ELEMENTS CONTAINING 20 w/o UO_2 IN A TYPE 318 PREALLOYED STAINLESS MATRIX

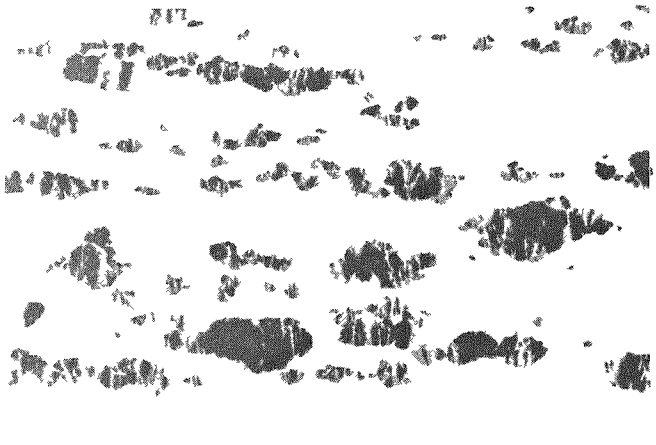

100X As Polished RM9412

a. 10 w/o Minus 100 Plus 140-Mesh-
90 w/o Minus 140 Plus 200-Mesh UO_2

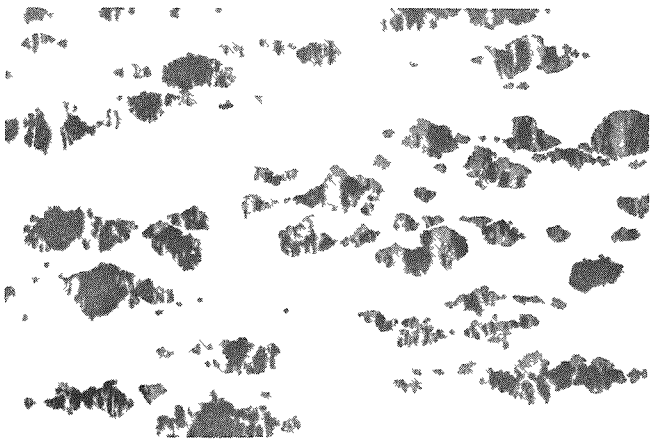

100X As Polished RM9415

b. 40 w/o Minus 100 Plus 140-Mesh-
60 w/o Minus 140 Plus 200-Mesh UO_2

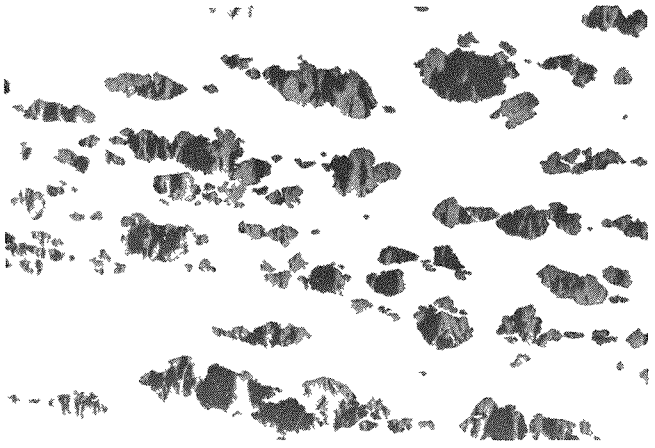

100X As Polished RM9416

c. 30 w/o Minus 100 Plus 140-Mesh-
40 w/o Minus 140 Plus 200-Mesh-
30 w/o Minus 200 Plus 270-Mesh UO_2

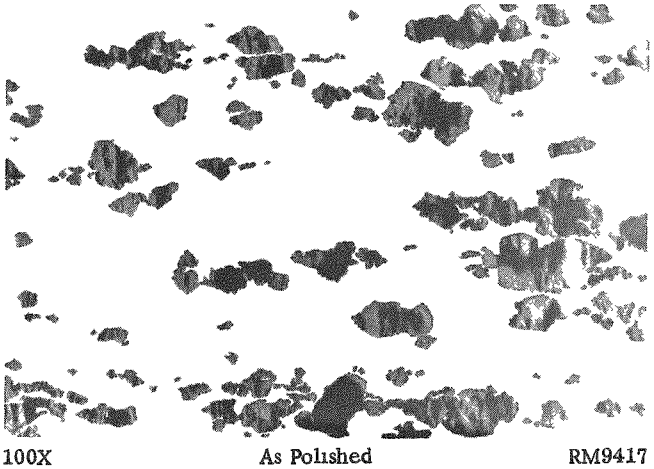

100X As Polished RM9417

d. 60 w/o Minus 100 Plus 140-Mesh-
20 w/o Minus 140 Plus 200-Mesh-
20 w/o Minus 200 Plus 270-Mesh UO_2

FIGURE 34. EFFECT OF UO_2 PARTICLE-SIZE VARIATION ON THE STRUCTURE OF 25 w/o UO_2 DISPERSED IN AN ELEMENTAL 18-14-2.5 ALLOY

As can be seen, particles of a wide range of sizes can be used to obtain good dispersions. Note, however, that the greatest percentage of UO_2 particles are relatively large.

UO_2 Loading

Stringering and fracturing of UO_2 particles became more severe as the UO_2 loading was increased. An example of the change in structure is shown in Figure 35. An increase in UO_2 loading also decreased tensile strength, transverse tensile strength, and bend ductility. Table 15 shows the effect of increased UO_2 loading on the transverse tensile strength.

TABLE 15. THE EFFECT OF UO_2 LOADING ON THE TRANSVERSE TENSILE STRENGTH OF UO_2-STAINLESS STEEL FUEL PLATES

UO_2, w/o	UO_2 Particle Size, μ	Core Matrix	Ultimate Tensile Strength[a], psi
15	75-150	Elemental 18-14-2.5 alloy	36,800
20	75-150	Elemental 18-14-2.5 alloy	32,500
25	75-150	Elemental 18-14-2.5 alloy	24,700
30	75-150	Elemental 18-14-2.5 alloy	21,900
35	75-150	Elemental 18-14-2.5 alloy	16,600
15	75-150	Prealloyed Type 318 stainless	29,000
25	50-75	Prealloyed Type 318 stainless	16,000
25	75-105	Prealloyed Type 318 stainless	15,400
30	75-150	Prealloyed Type 318 stainless	14,700
35	75-150	Prealloyed Type 318 stainless	11,200

(a) Values obtained at room temperature.

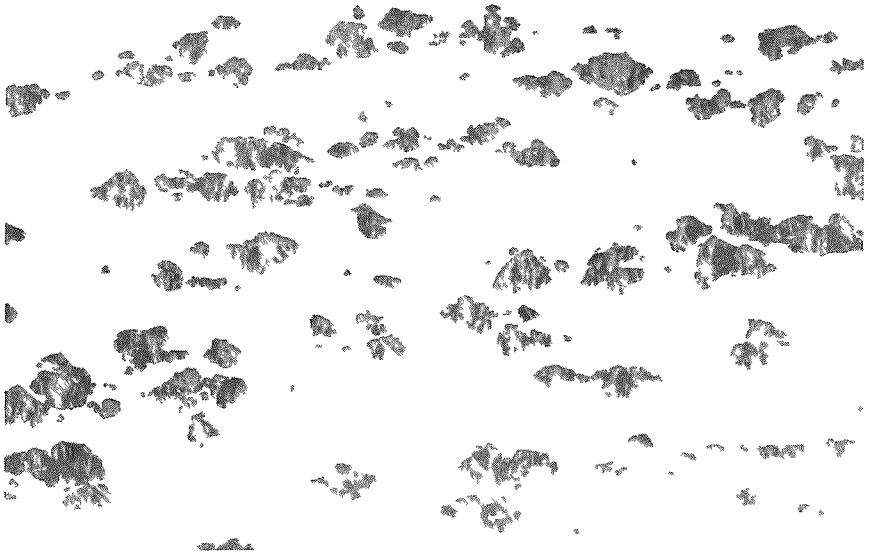

100X As Polished RM9040

a. 25 w/o UO_2

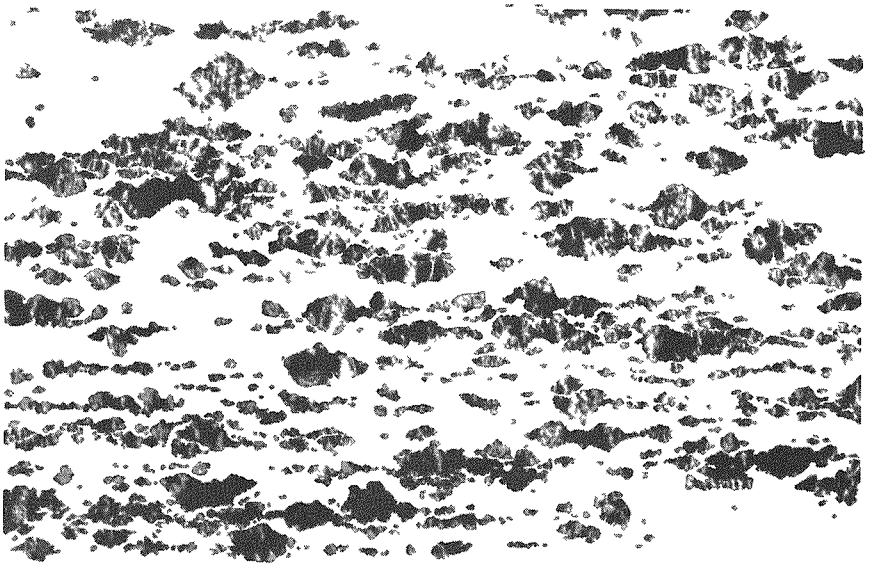

100X As Polished RM10007

b. 37 w/o UO_2

FIGURE 35. SEVERE STRINGERING AND FRACTURING RESULTING FROM AN INCREASED LOADING OF UO_2 IN AN ELEMENTAL 18-14-2.5 ALLOY

Type of UO_2

Four types of UO_2 were investigated. Use of Mallinckrodt ceramic-grade minus 325-mesh UO_2 was discontinued early in the program because of the sintering and crushing required to obtain powders of the correct particle size and also because the sintered particles did not appear to resist crushing during fabrication to the extent that Mallinckrodt Hi-Fired powder or Oak Ridge hydrothermal UO_2 did. Near the conclusion of the program Mallinckrodt spherical UO_2 became available and was investigated to a limited extent. As shown in Figure 36, a far more uniform dispersion with a negligible amount of stringering can be produced with spherical UO_2. As would be expected, the transverse tensile strength is also improved.

DISCUSSION OF RESULTS

A material with relatively high strength at 1500 to 1650 F, good corrosion resistance in oxidizing and nitriding atmospheres, and good ductility at room temperature was required for use in GCRE fuel elements. Type 318 stainless steel possesses these characteristics. Sigma phase will form after long periods of time at operating temperatures, but the good creep resistance at 1500 to 1650 F cannot be obtained in stainless steels which do not contain molybdenum (a sigma promoter). Furthermore, at the present time no conclusive evidence concerning detrimental effects of sigma on either irradiation resistance or mechanical properties has been offered. Limited data obtained in this investigation suggest that sigma may increase creep resistance.

However, from general considerations of radiation damage, it would be predicted that an austenitic stainless steel would have better resistance to radiation damage than a stainless steel containing two or three or four phases. Also, a material which contains a more uniform dispersion with less stringering and fracturing of UO_2 would be expected to have better resistance to irradiation. Although a high-temperature anneal is required (2300 F), the use of an elemental mixture of iron, chromium, nickel, and molybdenum more nearly meets these requirements than does prealloyed Type 318 stainless steel. Also, the effect of process variables on room-temperature ductility is much smaller and even neglible in the normal range of variations for elemental-powder-containing fuel elements. In addition, when compared with prealloyed-matrix fuel plates, hot tensile strength is always greater for elemental-powder-bearing fuel plates when measured in the transverse direction (thickness direction or transverse to rolling direction). The cross section of metal perpendicular to the applied force is more uniform when tension is applied in the rolling direction than in any other direction. Also, an added 30 volume per cent of metal is contributed by the cladding, and under these conditions the tensile strengths for fuel plates of both matrices fall within the same scatter band. If creep strength is the only criterion considered, the experimental results indicate that the prealloyed matrix is superior.

The major advantage usually cited for prealloyed powders is the fact that a homogeneous alloy can be easily obtained. While a homogeneous alloy is the result, a

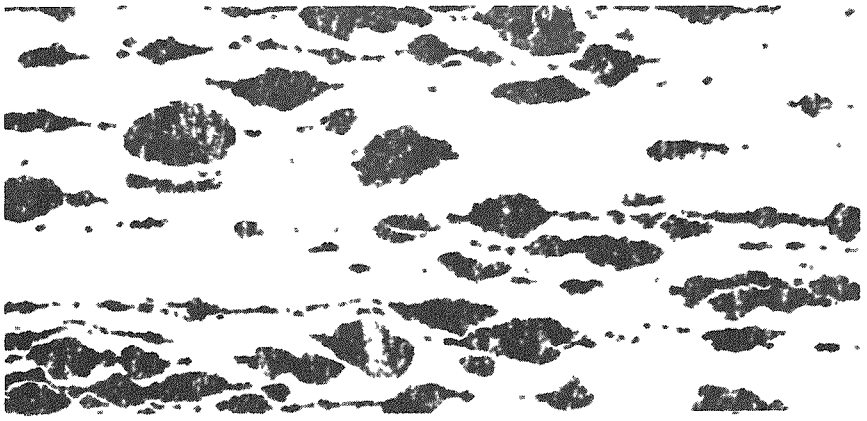

100X As Polished RM7417

a. Minus 100 Plus 200-Mesh Sintered Ceramic-Grade UO_2

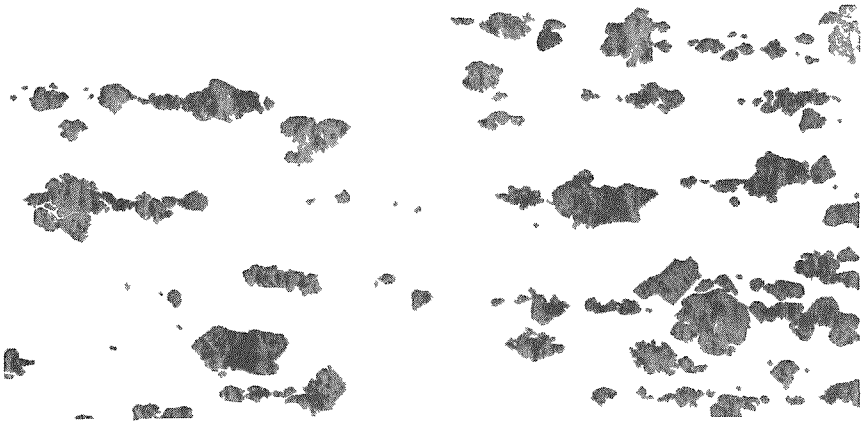

100X As Polished RM9039

b. Minus 140 Plus 200-Mesh Hi-Fired UO_2

100X As Polished RM11242

c. Minus 100 Plus 200-Mesh Spherical UO_2

FIGURE 36. EFFECT OF TYPE OF UO_2 ON STRUCTURE OF 25 w/o UO_2-ELEMENTAL MATRIX FUEL ELEMENTS

single-phase structure is not obtained. The results in this investigation indicate that it would be extremely difficult to obtain prealloyed-stainless-bearing fuel plates free of ferrite or sigma and, as in the wrought material, carbides will always be present. Furthermore, the techniques which have been developed for producing prealloyed-matrix fuel plates with good ductility, moderately good dispersion, and good transverse tensile strength closely approximate techniques used in making plates with elemental powders. Thus, many advantages cited for using prealloyed powders are lost when strict requirements are placed on mechanical properties or high service temperatures are contemplated.

Reliable methods have been developed for removing the two troublesome minor phases found in elemental-matrix plates (Cr_2O_3 and chromium-rich grains). Cold pressing at low pressures (15 to 30 tsi) and step sintering to 2300 F will remove all chromium oxide. The lower pressure is required if as-received electrolytic iron and electrolytic chromium are used, but the higher pressure is satisfactory when hydrogen-annealed electrolytic iron (approximately 2000 ppm oxygen) and Lunex chromium are used. A 2 to 4-hr anneal at 2300 F after hot or cold rolling will convert all chromium-rich areas into austenite.

Of the UO_2 powders investigated, the hydrothermal and Hi-Fired powders appear comparable, but the hydrothermal powder may be slightly more resistant to fracturing. The spherical UO_2 appears very promising but was not available in time to be completely investigated. Sintered ceramic-grade powder was used in the early work, but when better-quality powders in the desired particle size became available, use of this powder was discontinued.

Powder particle sizes were found to be important in determining the final core structure. Metal powders of minus 325 mesh were preferable whether elemental mixtures or prealloyed stainless powders were used. Variation of UO_2 particles over the range of 44 to 150 μ was not found to seriously affect the structure, but mechanical properties of prealloyed matrix plates appear to be sensitive to UO_2 particle size. Large particles (75 to 150 μ in diameter) are considered the most desirable.

The desired sintered density (85 per cent of theoretical) could be obtained over a wide variation of compacting pressure, UO_2 particle size, metal particle size, and UO_2 loading; therefore, the sintering process could be adjusted according to requirements for obtaining a good roll-clad structure without affecting the compact density. Of course, sintering techniques used for purposes such as removal of Cr_2O_3 were fixed within close limits.

Cold rolling produced more detrimental effects on the structure than any other roll-cladding operation. As little as an 8 per cent reduction in thickness produced some stringering and fracturing of UO_2 particles, and 30 per cent reduction in thickness caused moderately severe stringering and fracturing of UO_2. Approximately 15 to 20 per cent reduction in thickness was found to be necessary to produce the desired surface finish on the plates. Use of light passes for the reduction was found to be beneficial.

Hot rolling at 2200 F from a hydrogen atmosphere, with a 40 per cent reduction in thickness on the first pass and a 20 per cent reduction per pass on remaining passes

until a 6-to-1 up to a 7-to-1 total hot reduction was made, was found to be the most desirable procedure. However, because of overshadowing effects produced by cold rolling, variations from 30 to 50 per cent reduction in thickness on the first pass and variations from 2000 to 2200 F in rolling temperature did not produce severe changes in the final core structure. Decreasing the rolling temperature appears to be more detrimental than changing the rolling schedule.

A 2050 F anneal after cold rolling was necessary to tie up excess carbon in the form of niobium carbides and to give a flat, ductile plate.

CONCLUSIONS

Although the effect of single variables is listed below, the relative importance of each variable and its effect on other variables must be considered in establishing a fabrication process. Consideration of the factors listed below has resulted in the fabrication procedure listed in Appendix A.

(1) For fuel plates containing core matrices made from elemental iron, chromium, nickel, and molybdenum powders, only powders with a low impurity content, particularly oxygen content, and with a small particle size, $<44\ \mu$ in diameter (minus 325 mesh), should be used.

(2) The step-sintering process permits the use of electrolytic iron and chromium powder, carbonyl nickel powder, and hydrogen-reduced molybdenum powder as received from commercial sources, but the step-sintering technique can be simplified when hydrogen-reduced electrolytic iron and Lunex lithium-reduced chromium powder are used.

(3) Use of high-silicon prealloyed stainless steel powders can cause up to 20 volume per cent ferrite to be present after normal fabrication procedures.

(4) Use of low-silicon prealloyed stainless steel powders may cause the formation of up to 15 volume per cent chromite after normal fabrication procedures.

(5) The best properties are obtained for plates containing prealloyed powders when minus 325-mesh powder is used.

(6) Plates containing elemental matrices show consistently higher transverse tensile strength then plates containing prealloyed matrices.

(7) Microstructures show that better distribution of UO_2 and more uniform UO_2 particle size as well as an absence of secondary phases are obtained with plates made with elemental powders.

(8) Only by the use of minus 325-mesh metal powder and 100 to 150-mesh UO_2 were prealloyed matrix plates produced with a bend ductility equal to that for plates with elemental matrices.

(9) UO_2 particle size had little effect on bend ductility of elemental-matrix plates.

(10) Longitudinal tensile tests of clad plates at temperatures to 1650 F did not show significant differences due to use of elemental versus prealloyed matrices.

(11) Creep strength at 1500 and 1650 F was significantly higher for plates containing prealloyed matrices.

(12) Ferrite in Type 318 prealloyed-matrix plates transforms to sigma plus austenite after about 2 hr at 1500 F. After long periods of time (approximately 2000 hr at 1500 F) up to 10 volume per cent sigma in wrought stainless Type 318 and up to 5 volume per cent in elemental 18-14-2.5 matrices form by the transformation of austenite.

(13) Good dispersions can be produced by the use of either hydrothermal or Hi-Fired UO_2. Spherical UO_2 gave excellent results but was not fully investigated.

(14) Best results were obtained by the use of 75 to 150-μ-diameter UO_2 powder.

(15) A 2300 F anneal is required to place all chromium of elemental matrices in solution.

(16) A 2050 F anneal ties up excess carbon and results in plates with good room-temperature bend ductility.

REFERENCES

(1) Keeler, J. R., Keller, D. L., and Cuddy, L. J., "The Fabrication of Stainless Steel-Uranium Dioxide Fuel Elements", BMI-904 (March 2, 1954). Secret.

(2) Eudier, M., "The Sintering Mechanism of Pure Metals", Symposium on Powder Metallurgy, 1954, Special Report 58, Iron and Steel Institute, pp 59-63 (1956).

(3) Grobe, A. H., and Roberts, G. A., "Technology of Prealloyed Stainless Steel Powders", Prealloyed Steel Powder Bulletin No. 3, Vanadium Alloys Steel Co.

(4) Bain, E. C., et al., Trans. ASST, 21, 481-509 (1951).

(5) Holzworth, M. L., Beck, F. H., and Fontana, M. G., "The Mechanism of Knife-Line Attack in Welded Type 347 Stainless Steel", Corrosion, 7, 441-449 (1951).

(6) Simpkinson, T. V., "Behavior of Carbides in Niobium Stabilized Stainless Steels", Metallurgia, 47, 18-24 (1953).

(7) Symposium on the Nature, Occurrence, and Effects of Sigma Phase, ASTM Special Technical Publication No. 110 (1950).

(8) Aronson, A. "Investigations in the Sigma Fe-Cr-Si Systems", Acta Chem. Scan., 11, 365 (1957).

(9) Lena, A. J., "Sigma Phase – A Review", Metal Progress, 66, 94 (July, 1954); 86 (August, 1954); 122 (September, 1954).

SJP/DKL/GWC:ajk

APPENDIX A

RECOMMENDED PROCEDURE FOR FABRICATION OF UO_2-STAINLESS STEEL FUEL ELEMENTS

APPENDIX A

RECOMMENDED PROCEDURE FOR FABRICATION OF UO_2-STAINLESS STEEL FUEL ELEMENTS

The recommended fabrication technique presented below is for use with sintered cores containing elemental iron, nickel, chromium, and molybdenum powders. An identical procedure is used for prealloyed-matrix plates except for deletion of dry-metal powder blending and 2300 F heat treatment.

A. Preparation of Materials

(1) Shear cover plates to size and machine picture frames to a 25 rms surface. Material is Type 318 stainless steel.

(2) Clean components in alcohol or trichloroethylene, scrub with wire brush in hot soap solution, rinse in cold water, hot water, cold water, and pat dry with paper towels.

(3) Blend mixture of minus 325-mesh powders consisting of 18 w/o chromium, 14 w/o nickel, 2.5 w/o molybdenum, and the balance iron for 2 hr dry in a twin-shell blender. Add 25 w/o hydrothermal UO_2 (minus 100 plus 200-mesh size) and blend dry for 1 hr. Add 1/2 w/o camphor-alcohol binder and blend 1 hr. Note: as-received powders must be passed through a 325-mesh screen before blending.

B. Sintering

(1) Cold press core compact at 15 tsi.

(2) Sinter 2 to 16 hr at 1600 F (sinter until -90 F exit dew point is obtained), then heat at 170 F per hr to 2300 F and hold for 2 hr.

(3) Coin compacts at 50 tsi.

(4) Assemble billet components and Heliarc weld in a inert-gas-filled dry box.

(5) Evacuate pack at 600 F and seal by forging the evacuation stem closed.

C. Rolling

(1) Preheat billets and hot roll at 2200 F from a hydrogen-atmosphere muffle to an 80 per cent reduction in thickness. Reductions in thickness of 40 per cent per pass on the first pass and 20 per cent per pass on remaining passes are used.

(2) Pickle in HNO_3-HF-water bright etch to remove scale and anneal in a hydrogen atmosphere for 2 hr at 2300 F.

(3) Cold roll to a 15 to 20 per cent reduction in thickness using very light passes (3 per cent).

(4) Flat anneal 1 hr at 2050 F and cool in furnace cold zone.

APPENDIX B

PETROGRAPHIC ANALYSES OF UO_2 POWDERS

APPENDIX B

PETROGRAPHIC ANALYSES OF UO_2 POWDERS

Three types of UO_2 were examined for phase distribution, crystal grain size, porosity, and degree of crystallinity. The results for Hi-Fired UO_2, spherical UO_2, and hydrothermal UO_2 (fully enriched) are listed in Table B-1. A direct count of porosity for hydrothermal UO_2 was not made, but the examination indicated a porosity considerably less than 1 per cent.

TABLE B-1. POROSITY AND CRYSTAL GRAIN SIZE OF UO_2

Type of UO_2	Crystal Grain Size, μ			Number of Particles Measured	Total Direct Visual Porosity, volume per cent	Equivalent Water-Absorption Value
	Maximum	Minimum	Average			
Hi-Fired	100	2.5	19.6	100	1.96	0.49
Spherical	61	1.0	5.3	100	4.2	1.05
Hydrothermal	110	6.5	41.1	--	--	1.0

The degree of crystal-structure development and the relative perfection of crystal shape of the uranium oxide (UO_2) phase within the Hi-Fired UO_2 powder as received from the manufacturer appeared to suggest that the uranium oxide was made by a high-temperature calcination process. The major phase (95.9 volume per cent) consisted of isotropic crystal grains of isometric UO_2. A variety of crystal shapes could be detected.

The chemical identity of the secondary phase, which assisted in cementing the uranium oxide crystals together in the aggregate particles, could not be determined under the microscope but probably contained TiO_2. The secondary phase occurred as stringers in the interstices between the UO_2 crystals and as inclusions within the individual crystals. No evidence of birefringence was seen in polarized light. In general, the secondary phase was black and opaque in transmitted light.

The majority per cent of visual porosity at 1000X (diameters) magnification was confined to very small spherical-shaped pores that occurred within the individual crystals. A few narrow stringer-type channel pores were seen in the interstices between the UO_2 crystals. The aggregate particles appeared to be very compact and dense in structure. Therefore, there was little opportunity for elongated channel pores to be present.

The spherical UO_2 powder exhibited an unique aggregate particle structure. All of the aggregate particles were present as spheres of various sizes. Each sphere could contain several hundred small, brown crystals of the UO_2 phase. The small crystal grains were remarkably uniform in size. Brown aggregate highly predominated, but the presence of dark-colored aggregate probably contributed to the dark visual color of the powder as received from Mallinckrodt. Either the octahedron shape, a half-octahedron shape, or the triangular, octahedral crystal face predominated. Approximately 95.2 volume per cent of the sample was the UO_2 phase.

A number of dark chocolate-brown aggregates were seen. The amount was less than 5 per cent. The average crystal grain size in the dark aggregates was close to the average crystal grain size in the lighter brown aggregates. Any slight differences might be attributed to the presence of hidden phase impurities concealed within the space lattice of the UO_2 crystals in the dark aggregates. From the microscopic point of view, the amount of phase impurities necessary to produce a darker aggregate could not be determined. A few coarse crystals were seen in the powder and a number of dark crystals were counted.

The hydrothermal UO_2 appeared to have been made in the electric furnace using a fusion method, although the precipitation from UO_2 hydrate was actually used. Therefore, the space lattice within the uranium oxide crystals is set and well defined. A careful inspection of the sample failed to disclose the presence of measurable percentages of extraneous material.

Examination of the fine powder in reflected light revealed that nearly all of the crystals were dark and nearly black in color. A few crystals were clear and yellow brown in appearance. Although only 92.2 volume per cent of the UO_2 phase was measured, the secondary phase was also isotropic and the index of refraction indicated that the composition was very near that of pure UO_2. No evidence of impurities was detected.

SJP:DLK:GWC/ajk